Andean Geology 37 (2): 375-397. July, 2010

Andean Geology
formerly Revista Geológica de Chile
www.scielo.cl/andgeol.htm

Permian depositional age of metaturbidites of the Duque de York Complex, southern Chile: U-Pb SHRIMP data and palynology

Fernando A. Sepúlveda[1], Sylvia Palma-Heldt[2], Francisco Hervé[3], C. Mark Fanning[4]

[1] *Servicio Nacional de Geología y Minería, Av. Santa María 0104, Santiago, Chile.*
fsepulveda@sernageomin.cl; fersepul@ing.uchile.cl

[2] *Departamento de Ciencias de la Tierra, Universidad de Concepción, Barrio Universitario S/N°, Concepción, Chile.*
sypalma@udec.cl

[3] *Departamento de Geología, Universidad de Chile, Casilla 13518, Correo 21, Santiago, Chile.*
fherve@ing.uchile.cl

[4] *Research School of Earth Sciences, The Australian National University, Mills Road, Canberra, ACT 0200, Australia.*
Mark.Fanning@anu.edu.au

ABSTRACT. The Duque de York Complex (DYC) is part of the low grade metamorphic accretionary complexes of the pre-Andean Patagonian 'basement'. It is a sedimentary succession exposed along the western margin of southernmost South America. New U-Pb zircon ages and palynological data restrict the maximum depositional age of the DYC to the limit between the early Permian (Kungurian) and the middle Permian (Roadian). The palynological association recorded in the DYC, characterized mainly by Gymnospermopsida pollen, indicates a humid environment of forest with an undergrowth of ferns. Regional paleogeographic correlations point out that an interpretation of DYC as an autochthonous terrane cannot be discarded, contrasting with previous hypotheses which suggest an allochthonous character for this complex.

Keywords: Palynology, U-Pb dating, Duque de York Complex, Terranes, Gondwana, Chile.

RESUMEN. Edad pérmica de sedimentación de las metaturbiditas del Complejo Duque de York, sur de Chile: datos mediante U-Pb SHRIMP y palinología. El Complejo Duque de York (CDY) forma parte de los complejos metamórficos acrecionarios del 'basamento' pre-Andino de la Patagonia, correspondiendo a una sucesión sedimentaria que aflora a lo largo del margen occidental austral de Sudamérica. Nuevas edades U-Pb en circón, en combinación con información palinológica, permiten acotar la máxima edad de depósito posible del CDY al límite entre el Pérmico temprano (Kunguriano) y el Pérmico medio (Roadiano). La asociación palinológica registrada en el CDY está caracterizada por Gymnospermopsida, e indica un ambiente húmedo de bosque con sotobosque de helechos. Las correlaciones paleogeográficas apuntan a que la condición de terreno autóctono del CDY no puede ser descartada, lo que se contrapone a hipótesis anteriores, las que sugieren un carácter alóctono para este complejo.

Palabras clave: Palinología, Datación U-Pb, Complejo Duque de York, Terrenos, Gondwana, Chile.

1. Introduction

The Duque de York Complex (DYC) is one of the metamorphic complexes that form the pre-Andean Patagonian 'basement' rocks, which crop out extensively along the western edge of South America south of 50°S. These rocks have been generally considered as part of the late Paleozoic-early Mesozoic accretionary prism built at the paleo-Pacific (Panthalassan) margin of Gondwana (*e.g.*, Hervé *et al.*, 1981; Forsythe, 1982). The accretionary orogenic belt that formed on this margin is one of the largest known orogenic belts in Earth history, and now occupies the eastern third of Australia, New Zealand, West Antarctica, the Transantarctic Mountains and large parts of southern South America (Vaughan *et al.*, 2005). This orogenic belt has been termed in two different ways depending on the interval considered: the Proterozoic and Paleozoic Terra Australis orogen (Cawood, 2005), and the Paleozoic and Mesozoic Australides (Vaughan *et al.*, 2005). It has been regarded as a collage of accreted terranes-terranes being fault-bounded packages of rocks of regional extent characterized by a geological history that differs from that of neighboring terranes (Howell *et al.*, 1985; Vaughan *et al.*, 2005).

The DYC corresponds to a widespread low grade-metasedimentary succession that crops out along the Madre de Dios and Diego de Almagro archipelagos (50°00'-51°50'S) and at the Ramírez, Contreras and Desolación islands (51°50'-53°00'S), in southern Chile (Fig. 1A). Forsythe and Mpodozis (1979, 1983) interpreted the DYC as a continent-derived detrital succession that was deposited over two coeval late Paleozoic exotic oceanic units, as they approached the continental margin of Gondwana. The DYC together with the oceanic units, defined as the Madre de Dios Accretionary Complex (MDAC) by Thomson and Hervé (2002), were then tectonically amalgamated to the forearc of this margin by subduction processes, resulting in an intricate tectonic interweaving. These complexes were intruded by the South Patagonian Batholith (SPB) in the Early Cretaceous (Halpern, 1973; Duhart *et al.*, 2003; Hervé *et al.*, 2007a).

For a long time, the accretionary complexes that compose the MDAC have been considered of exotic or allochthonous origin, or at least, as suspect terranes. Terranes are 'suspect' if there is doubt about their paleogeographical setting with respect to adjacent terranes or continental margin (Coney *et al.*, 1980; Coombs, 1997), and may be described as 'exotic', 'far-travelled' or 'allochthonous' (all meaning about the same thing) if there is sufficient evidence that they originated far from their present locations, often assumed to be hundreds or thousands of kilometers away (Vaughan *et al.*, 2005). The consideration of the MDAC as suspect and potentially exotic is based mainly on its fossil content and the inferred depositional setting for them (in the case of the TL and the coeval DC) (*e.g.*, Ling *et al.*, 1985; Ramos, 1988) and on the impossibility to find a contemporaneous magmatic arc as the source of Permian zircons for the DYC anywhere at a similar latitude in southern Patagonia (Hervé *et al.*, 2003; Hervé and Mpodozis, 2005; Hervé *et al.*, 2006). The latter has led to propose that the deposition of the DYC took place at high southern latitudes along the Antarctic sector of the Gondwana margin (Lacassie, 2003; Lacassie *et al.*, 2006). However, derivation of the DYC from lower and warmer latitudes is a hypothesis that cannot be ruled-out.

The lack of index fossils in the DYC has prevented an accurate determination of the depositional age of this complex. In consequence, a late early Permian maximum depositional age has been established by the use of the youngest detrital zircon population in these metasediments (Hervé *et al.*, 2003). Nevertheless, the use of the youngest detrital zircon age or population in a sediment as a limit for the age of deposition has been questionable for both geological (there is no necessary connection between the timing of zircon-generating events in a source region and the age of final deposition of a sediment eroded from this source) and statistical reasons (Andersen, 2005). In this context, this paper presents the first palynological study in rocks of the DYC and it also corresponds to the first record of late Paleozoic palynomorphs in Chile. The aim of this work is to restrict the age range of the DYC by the combination of the palynological results with new U-Pb SHRIMP ages in key samples, and also gives a revision of the paleoenvironmental and geochronological data regarding the place and timing of deposition of the DYC. The conclusions derived from this work allow giving some new considerations focused on the supposed allochthonous character of the MDAC, and especially of the DYC.

2. Geological background

The rocks of the studied area were first recognized by Cecioni (1955, 1956), who determined

the presence of upper Paleozoic sediments in the Patagonian archipelago, distinguishing fusulinids as well as the low grade-metamorphic character of these rocks. The geology of the Madre de Dios Archipelago was studied in detail by Forsythe and Mpodozis (1979, 1983) and Mpodozis and Forsythe (1983), who distinguished three metamorphic complexes that made up the MDAC (Fig. 1B):

a. the Denaro Complex (DC), formed by tholeiitic basalts with E- and N-MORB signatures (Hervé *et al.*, 1999; Sepúlveda *et al.*, 2008), banded radiolarian and metalliferous cherts, pelites and calcarenites. This complex represents fragments of ocean floor and its sedimentary cover (late Carboniferous-early Permian, according to Ling *et al.*, 1985),

b. the Tarlton Limestones (TL), formed by fusulinid-bearing massive limestones, deposited in an intra-oceanic carbonate platform during Middle Pennsylvanian-early Permian times (Cecioni, 1956; Douglass and Nestell, 1972, 1976),

c. the Duque de York Complex (DYC), formed by a thick succession of greywackes, pelites, and minor conglomerates of continental provenance, and deposited on top of DC and TL. Based on field observation, Faúndez *et al.* (2002) described the DYC as being formed by metaturbidites. Also, it has been indicated that this succession has early Permian radiolarian cherts at Desolación Island (A. Yoshiaki, written communication, 2002; in Hervé *et al.*, 2007b). Owing to the accretionary processes, most contacts among these units are of tectonic

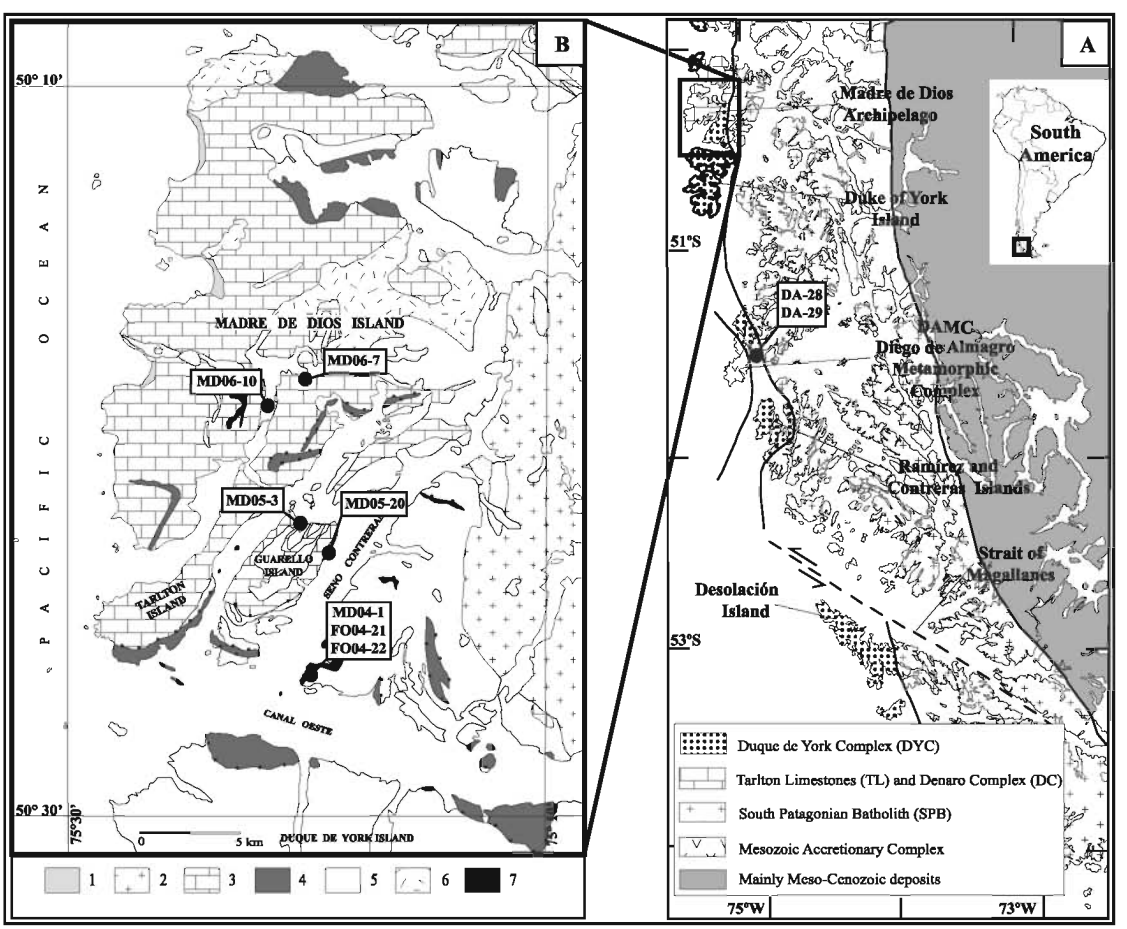

FIG. 1. **A.** Sketch map showing the distribution of the DYC; **B.** Geological map of the Madre de Dios Archipelago (after Forsythe and Mpodozis, 1983; Lacassie *et al.*, 2006; Sepúlveda *et al.*, 2008). **1.** Quaternary deposits; **2.** South Patagonian Batholith (SPB); **3.** Tarlton Limestones (TL); **4.** Denaro Complex (DC); **5.** Duque de York Complex (DYC); **6.** Unmapped basement; **7.** Sill. Sampling sites are marked with black circles; all for palynology except FO04-21; FO04-21 and FO04-22 for U-Pb Shrimp dating.

origin (Fig. 2), but few examples of depositional contacts have been recognized. In fact, the preserved stratigraphic relations confirm that the DYC has both unconformable and conformable depositional contacts with the other complexes (*e.g.*, Lacassie *et al.*, 2006).

All these units where metamorphosed under the conditions of pumpellyite-actinolite facies in a frontal accretionary wedge (Sepúlveda, 2004; Sepúlveda *et al.*, 2008) during Middle Triassic to earliest Jurassic times, as indicated by *in situ* Ar/Ar UV-LAMP ages on phengites (Willner *et al.*, 2009). Thomson and Hervé (2002) used zircon fission track data to point out that the metamorphism that affects the DYC, and also the underlying TL and DC, took place during or before the earliest Jurassic (*ca.* 195 Ma). This information constrains the minimum probable age of deposition for the DYC, and demonstrates that, in this area, the metamorphism occurred prior to the emplacement of the SPB in the Early Cretaceous. The isotopic ages of the SPB, in the outcrops adjacent to the contact with the MDAC, are 133-112 Ma (Rb-Sr whole rock and biotite isochron, Halpern, 1973), 130-143 Ma (K-Ar biotite, Duhart *et al.*, 2003) and *ca.* 133 Ma (U-Pb SHRIMP zircon, Hervé *et al.*, 2007a).

U-Pb SHRIMP detrital zircon ages from sandstones of the DYC reveal that the youngest main opulation, and hence the maximum possible depositional age, is late early Permian (*ca.* 270 Ma) (Hervé *et al.*, 2003). The geochemical study of Lacassie *et al.* (2006), complementing the data and refining the conclusions of Faúndez *et al.* (2002), indicates that the DYC sandstones and mudstones had their source in a volcanic arc of granodioritic average composition located relatively proximal to the depositional basin, and whose plutonic roots had been exposed by erosion. Also, they propose that the DYC was deposited in a tectonic setting corresponding to an active continental margin, possibly located along the Antarctic segment of the Panthalassan Gondwana margin.

FIG. 2. Outcrops at Madre de Dios Island, where tectonic contact (dashed line) between deformed metasediments of the DYC (brown) and massive limestones of the TL (white) is partly observed.

2.1. Paleogeographic setting

The fusulinid fauna in the TL shows that these carbonate sedimentary rocks must have been deposited in marine warm water (Douglass and Nestell, 1976). Similarities between the fossil content of the TL with those of the backarc marine carbonate deposits of the late Paleozoic Copacabana Formation in Peru and Bolivia (Cabrera La Rosa and Petersen, 1936; Chamot, 1965; Mamet, 1996), indicates that deposition of TL occurred in low latitude zones (*ca.* 20°S) during the late Carboniferous-early Permian (Lacassie, 2003). However, recent paleogeographic reconstructions for those periods (Torsvik and Cocks, 2004; Veevers, 2004; Cocks and Torsvik, 2006; Cawood and Buchan, 2007) locate the portion of the Gondwana margin where the Madre de Dios archipelago is presently situated at a high southern latitude, well outside the tropical zone where the TL is likely to have been deposited. Also, it is indicated that the late Paleozoic Ice Age in Gondwana was active between the Carboniferous and the early Permian (Isbell *et al.*, 2003; Isbell *et al.*, 2005; López-Gamundí, 2005; Buatois *et al.*, 2006; Fielding *et al.*, 2008; Rocha Campos *et al.*, 2008). These facts, together with the contemporaneity of the TL with the ocean floor deposit of the DC (Ling *et al.*, 1985; Ling

and Forsythe, 1987) lead to the conclusion that the MDAC represents an allochthonous or exotic terrane derived from lower latitudes and accreted via subduction processes to Gondwana (Ramos, 1988). The timing of the accretion of these units would be bracketed between the maximum age of deposition of the DYC (*ca.* 270 Ma; Hervé *et al.*, 2003) and the minimum age of metamorphism (195 Ma; Thomson and Hervé, 2002).

The apparent lack of a Permian magmatic arc in southernmost Patagonia allowed Lacassie (2003) and Lacassie *et al.* (2006), following Hervé *et al.* (2000) and Cawood *et al.* (2002), to propose that the accretion of the TL and the DC would have occurred against the Antarctic-Australian segment of the Gondwana margin, from where both would have been displaced by dextral translation, together with the DYC, as a coherent block to their current position. In addition, Lacassie *et al.* (2006) show that the DYC metasediments share important petrographic, geochemical and geochronological characteristics with metaturbidites present in the Rakaia Terrane in New Zealand and with the eastern (Triassic) Le May Group in Alexander Island. These similarities point towards similar igneous sources for the three successions, suggesting that they were coevally deposited along the same active continental margin (Lacassie *et al.*, 2006). This margin was probably located along the Antarctic sector of the Panthalassan Gondwana margin, as favored by the studies of Willan (2003) for the source area of the Le May Group, and of Wandres *et al.* (2004) and Wandres and Bradshaw (2005) for the source area of the Rakaia terrane. The last two studies indicate that the origin of the Permian detritus in the Rakaia terrane would be in the igneous rocks of the Amundsen and Ross Provinces, East Antarctica, which during the Permian were close to 60°S (Veevers, 2004; Cawood and Buchan, 2007). If the source of Permian detritus was the same for these three successions (DYC, Rakaia Terrane and Le May Group), this would imply dextral strike-slip displacement of the MDAC along the SW Gondwana margin from these high latitude to its present position.

On the other hand, paleomagnetic information on the TL and the DC demonstrate that, after Early Cretaceous remagnetization produced by the thermal influence of the SPB, both units underwent a counter-clockwise rotation of *ca.* 117° with an inappreciable latitudinal change (Rapalini *et al.*, 2001). This evidence, coupled to the structural data of Forsythe and Mpodozis (1979, 1983), allowed Rapalini *et al.* (2001) to propose that the former units have been accreted to the Gondwana margin from the NW rather than from the SW, as had been previously considered (Forsythe and Mpodozis, 1983; Ling and Forsythe, 1987). That agrees with the early hypothesis of Ozawa and Kanmera (1984), which suggested the north-western Pacific area for the origin of the exotic oceanic units of the MDAC, and is also consistent with the sinistral sense of shear of main structures parallel to the margin of South America (Cunningham, 1993; Olivares *et al.*, 2003). These interpretations are coherent with the migration of the Antarctic Peninsula towards the south starting in the latest Jurassic (Hervé *et al.*, 2006; König and Jokat, 2006; Miller, 2007), which was situated parallel to the west of Patagonia at that time (Miller, 2007, and references therein). Moreover, it is suggested that the late Triassic deformation in northern Antarctic Peninsula (Peninsula Orogeny), which affects the Trinity Peninsula Group accretionary complex (TPG, Hyden and Tanner, 1981), is associated with sinistral strike-slip movements, while dextral strike-slip is mainly a Cretaceous phenomenon in the Antarctic Peninsula (written communication, A. Vaughan, October 2006).

The deposition of sediments of the DYC in high southern latitudes (Lacassie, 2003; Lacassie *et al.*, 2006), contrasts with the second scenario, which involves deposition of the DYC in lower and warmer latitudes, perhaps associated with subsequent sinistral strike-slip movements of the entire MDAC along the Panthalassan margin of Gondwana.

3. Sampling and Methods

Palynological data were acquired from one sample of limestone of the TL and seven samples of metasediments of the DYC: five from Madre de Dios Archipelago and two from Diego de Almagro Archipelago (Table 1; Fig. 1). All samples were processed by standard palynological methods. All but one of the samples (MD05-20 from Guarello Island) yielded poorly preserved palynomorphs. The study and the description of the specimens were made with an optical microscope. The slides are housed at the Laboratory of Paleopalynology of the Departamento de Ciencias de la Tierra, Universidad de Concepción under codes 1396 to 1401.

Two metasedimentary samples (FO04-21 and FO04-22) from the units of the MDAC were collected for U-Pb zircon dating by SHRIMP RG (sensitive high resolution ion microprobe, reverse geometry) at the Research School of Earth Sciences, The Australian National University. Zircon grains were separated from total rock samples using standard crushing, washing, heavy liquid and paramagnetic procedures. The zircon-rich heavy mineral concentrates were poured onto double-sided tape, mounted in epoxy together with chips of the reference zircons (FC1 and SL13), sectioned approximately in half, and polished. Reflected and transmitted light photomicrographs were prepared for all zircons. Cathodoluminescence (CL) Scanning Electron Microscope (SEM) images were prepared for all zircon grains. The CL images were used to decipher the internal structures of the sectioned grains and to ensure that the ~20 μm SHRIMP spot was wholly within a single age component (usually the youngest) within the sectioned grains.

The U-Th-Pb analyses were made using SHRIMP RG. The zircon grains were analyzed sequentially and randomly. Each analysis consisted of 4 scans through the mass range, with a reference zircon analyzed for every five unknown zircon analyses; SHRIMP analytical method follows Williams (1998, and references therein). The data have been reduced using the SQUID Excel Macro of Ludwig (2001). The U-Pb ratios have been normalized relative to a value of 0.01859 for the FC1 reference zircon, equivalent to an age of 1,099 Ma (Paces and Miller, 1993). Uncertainties given for individual analyses (ratios and ages) are at the one sigma level (Tables 2 and 3). Tera-Wasserburg concordia plots, probability density plots with stacked histograms and weighted mean $^{206}Pb/^{238}U$ age calculations were carried out using ISOPLOT/EX (Ludwig, 2003). The 'Mixture Modelling' algorithm of Sambridge and Compston (1994), via ISOPLOT/EX, was used to un-mix statistical age populations or groupings; from these groups weighted mean $^{206}Pb/^{238}U$ ages were calculated and the uncertainties are reported as 95% confidence limits.

An estimate for the maximum age for the deposition of the sediment sample may be determined from the weighted mean age of the youngest peak in these distributions, where ≥3 analyses are within analytical uncertainty. Such an age grouping has taken into account isolated cases of inferred radiogenic Pb-loss, which can produce minor scatter to younger ages. Ages for individual grains are reported at the 68% confidence level, and Geological Time Scale referred throughout the text is that of Gradstein *et al.* (2004).

TABLE 1. SAMPLES ANALYZED BY PALYNOLOGICAL METHODS.

Sample	Lithology (unit)	Location (coordinates)
MD04-1	black shale (DYC)	50°25'43.2"S; 75°19'33.1"W
FO04-22	sandstone (DYC)	50°25'43.2"S; 75°19'33.1"W
MD05-3	calcareous sandstone (DYC)	50°21'54.1"S; 75°19'53.8"W
MD05-20	sandstone (DYC)	50°22'46.4"S; 75°19'01.1"W
MD06-7	limestone (TL)	50°18'14.2"S; 75°20'17.2"W
MD06-10	sandstone (DYC)	50°19'07.6"S; 75°21'50.1"W
DA-28	sandstone (DYC)	51°30'40.5"S; 75°06'21.3"W
DA-29	shale (DYC)	51°30'40.5"S; 75°06'21.3"W

TABLE 2. ANALYTICAL DATA FOR SAMPLE FO04-21 (SUMMARY OF SHRIMP U-Pb ZIRCON RESULTS FOR SAMPLE FO04-21).

							Total Ratios				Radiogenic Ratios							Age (Ma)				
Grain. spot	U (ppm)	Th (ppm)	Th/U	$^{206}Pb^*$ (ppm)	$^{204}Pb/^{206}Pb$	f_{206} %	$^{238}U/^{206}Pb$	±	$^{207}Pb/^{206}Pb$	±	$^{206}Pb/^{238}U$	±	$^{207}Pb/^{235}U$	±	$^{207}Pb/^{206}Pb$	±	ρ	$^{206}Pb/^{238}U$	±	$^{207}Pb/^{206}Pb$	±	% Disc
1.1	124	88	0.71	14.1	0.000174	0.30	7.576	0.107	0.0743	0.0013	0.1316	0.0019	1,302	0.039	0.0718	0.0019	0.477	797	11	980	53	19
2.1	485	128	0.26	35.6	0.000071	0.36	11.687	0.139	0.0609	0.0008	0.0853	0.0010	-	-	-	-	-	527	6	-	-	-
3.1	762	419	0.55	29.8	0.001414	0.80	21.953	0.258	0.0584	0.0009	0.0452	0.0005	-	-	-	-	-	285	3	-	-	-
4.1	581	181	0.31	68.9	-	<0.01	7.249	0.082	0.0681	0.0006	0.1380	0.0016	1,295	0.018	0.0681	0.0006	0.802	833	9	871	17	4
5.1	841	551	0.66	29.8	0.000092	0.06	24.213	0.276	0.0519	0.0008	0.0413	0.0005	-	-	-	-	-	261	3	-	-	-
7.1	787	507	0.64	30.0	0.001116	0.52	22.506	0.265	0.0560	0.0009	0.0442	0.0005	-	-	-	-	-	279	3	-	-	-
8.1	877	556	0.63	33.4	0.000741	0.90	22.559	0.265	0.0590	0.0008	0.0439	0.0005	-	-	-	-	-	277	3	-	-	-
9.1	780	460	0.59	29.0	0.000093	0.06	23.092	0.265	0.0522	0.0008	0.0433	0.0005	-	-	-	-	-	273	3	-	-	-
10.1	546	493	0.90	25.6	0.006618	8.20	18.354	0.237	0.1186	0.0038	0.0500	0.0007	-	-	-	-	-	315	4	-	-	-
13.1	672	528	0.79	36.8	0.005147	6.39	15.673	0.215	0.1056	0.0032	0.0597	0.0009	-	-	-	-	-	374	5	-	-	-
14.1	654	702	1.07	25.4	0.003302	5.34	22.121	0.272	0.0945	0.0019	0.0428	0.0005	-	-	-	-	-	270	3	-	-	-
15.1	446	328	0.73	24.4	0.003231	5.35	15.691	0.266	0.0973	0.0028	0.0603	0.0011	-	-	-	-	-	378	6	-	-	-
16.1	744	360	0.48	27.5	0.000033	0.16	23.279	0.270	0.0529	0.0008	0.0429	0.0005	-	-	-	-	-	271	3	-	-	-
17.1	542	265	0.49	19.5	0.000162	0.29	23.890	0.304	0.0539	0.0009	0.0417	0.0005	-	-	-	-	-	264	3	-	-	-
18.1	363	237	0.65	13.6	0.000832	1.68	22.987	0.296	0.0651	0.0013	0.0428	0.0006	-	-	-	-	-	270	3	-	-	-
21.1	1,037	674	0.65	42.2	0.001689	2.52	21.130	0.239	0.0723	0.0009	0.0461	0.0005	-	-	-	-	-	291	3	-	-	-
22.1	322	3	0.01	20.7	-	<0.01	13.351	0.168	0.0556	0.0010	0.0750	0.0010	-	-	-	-	-	466	6	-	-	-
23.1	602	186	0.31	28.4	0.000255	0.63	18.224	0.215	0.0584	0.0010	0.0545	0.0007	-	-	-	-	-	342	4	-	-	-
24.1	742	425	0.57	29.4	0.002074	3.21	21.650	0.252	0.0777	0.0022	0.0447	0.0005	-	-	-	-	-	282	3	-	-	-
25.1	676	342	0.50	38.9	0.000408	5.01	14.941	0.171	0.0951	0.0010	0.0636	0.0007	-	-	-	-	-	397	5	-	-	-
26.1	365	250	0.69	14.2	0.000298	0.86	22.118	0.287	0.0588	0.0012	0.0448	0.0006	-	-	-	-	-	283	4	-	-	-
27.1	787	137	0.17	58.1	0.000059	<0.01	11.644	0.129	0.0569	0.0006	0.0860	0.0010	-	-	-	-	-	532	6	-	-	-
28.1	860	167	0.19	82.3	0.000021	0.43	8.977	0.116	0.0656	0.0005	0.1109	0.0015	-	-	-	-	-	678	9	-	-	-
29.1	611	315	0.52	23.2	0.002652	4.70	22.608	0.268	0.0893	0.0012	0.0422	0.0005	-	-	-	-	-	266	3	-	-	-
30.1	201	134	0.67	8.2	0.000390	1.35	20.973	0.322	0.0631	0.0018	0.0470	0.0007	-	-	-	-	-	296	5	-	-	-
31.1	575	306	0.53	21.6	0.000503	0.77	22.824	0.278	0.0579	0.0010	0.0435	0.0005	-	-	-	-	-	274	3	-	-	-
32.1	650	467	0.72	25.2	0.004512	7.12	22.140	0.263	0.1087	0.0014	0.0419	0.0005	-	-	-	-	-	265	3	-	-	-
33.1	690	389	0.56	25.8	0.000172	0.21	22.998	0.271	0.0534	0.0009	0.0434	0.0005	-	-	-	-	-	274	3	-	-	-
34.1	827	576	0.70	31.3	-	<0.01	22.675	0.260	0.0506	0.0008	0.0442	0.0005	-	-	-	-	-	279	3	-	-	-
35.1	891	533	0.60	32.6	0.000322	0.40	23.521	0.269	0.0548	0.0008	0.0423	0.0005	-	-	-	-	-	267	3	-	-	-

Table 2 continued.

							Total Ratios				Radiogenic Ratios							Age (Ma)				
Grain. spot	U (ppm)	Th (ppm)	Th/U	$^{206}Pb^*$ (ppm)	$^{204}Pb/^{206}Pb$	f_{206} %	$^{238}U/^{206}Pb$	±	$^{207}Pb/^{206}Pb$	±	$^{206}Pb/^{238}U$	±	$^{207}Pb/^{235}U$	±	$^{207}Pb/^{206}Pb$	±	ρ	$^{206}Pb/^{238}U$	±	$^{207}Pb/^{206}Pb$	±	% Disc
36.1	636	291	0.46	25.0	0.001799	2.96	21.821	0.260	0.0756	0.0011	0.0445	0.0005	-	-	-	-	-	280	3	-	-	-
37.1	583	300	0.51	21.7	0.000215	0.21	23.073	0.280	0.0534	0.0010	0.0432	0.0005	-	-	-	-	-	273	3	-	-	-
38.1	871	562	0.64	32.0	0.000364	0.01	23.365	0.267	0.0518	0.0008	0.0428	0.0005	-	-	-	-	-	270	3	-	-	-
40.1	883	453	0.51	33.9	0.000032	0.07	22.399	0.361	0.0525	0.0008	0.0446	0.0007	-	-	-	-	-	281	4	-	-	-
41.1	551	332	0.60	20.5	0.000145	<0.01	23.101	0.284	0.0516	0.0010	0.0433	0.0005	-	-	-	-	-	273	3	-	-	-
42.1	663	408	0.62	25.1	0.000693	1.02	22.727	0.290	0.0600	0.0010	0.0436	0.0006	-	-	-	-	-	275	3	-	-	-
43.1	257	124	0.48	9.7	0.000159	0.10	22.823	0.331	0.0526	0.0015	0.0438	0.0006	-	-	-	-	-	276	4	-	-	-
44.1	1,081	984	0.91	43.2	0.001981	2.62	21.529	0.248	0.0730	0.0009	0.0452	0.0005	-	-	-	-	-	285	3	-	-	-
45.1	685	419	0.61	25.2	-	<0.01	23.388	0.280	0.0509	0.0009	0.0428	0.0005	-	-	-	-	-	270	3	-	-	-
46.1	398	372	0.94	14.1	0.000162	0.12	24.316	0.294	0.0524	0.0009	0.0411	0.0005	-	-	-	-	-	260	3	-	-	-
47.1	161	98	0.61	6.2	0.002612	4.12	22.090	0.304	0.0848	0.0021	0.0434	0.0006	-	-	-	-	-	274	4	-	-	-
48.1	678	406	0.60	25.0	0.000017	0.17	23.350	0.272	0.0530	0.0006	0.0428	0.0005	-	-	-	-	-	270	3	-	-	-
49.1	471	193	0.41	17.2	0.000050	0.18	23.511	0.283	0.0531	0.0008	0.0425	0.0005	-	-	-	-	-	268	3	-	-	-
50.1	789	272	0.34	35.5	0.000032	0.21	19.092	0.229	0.0547	0.0006	0.0523	0.0006	-	-	-	-	-	328	4	-	-	-
51.1	300	65	0.22	16.2	0.000259	0.03	15.946	0.196	0.0548	0.0008	0.0627	0.0008	-	-	-	-	-	392	5	-	-	-
52.1	126	134	1.06	4.7	-	<0.01	23.209	0.342	0.0509	0.0015	0.0431	0.0006	-	-	-	-	-	272	4	-	-	-
53.1	586	288	0.49	21.5	0.000029	0.06	23.471	0.271	0.0521	0.0006	0.0426	0.0005	-	-	-	-	-	269	3	-	-	-
54.1	455	324	0.71	17.0	0.001647	2.82	23.028	0.271	0.0742	0.0009	0.0422	0.0005	-	-	-	-	-	266	3	-	-	-
55.1	684	401	0.59	25.4	0.000077	<0.01	23.123	0.265	0.0511	0.0006	0.0433	0.0005	-	-	-	-	-	273	3	-	-	-
56.1	601	260	0.43	21.5	0.000064	0.02	24.071	0.282	0.0517	0.0007	0.0415	0.0005	-	-	-	-	-	262	3	-	-	-
57.1	733	436	0.60	26.4	0.000083	0.11	23.838	0.282	0.0524	0.0007	0.0419	0.0005	-	-	-	-	-	265	3	-	-	-
58.1	940	193	0.21	35.2	0.001162	1.98	22.941	0.265	0.0675	0.0013	0.0427	0.0005	-	-	-	-	-	270	3	-	-	-
59.1	1,770	2,148	1.21	60.3	0.000014	0.11	25.237	0.283	0.0521	0.0004	0.0396	0.0004	-	-	-	-	-	250	3	-	-	-
60.1	629	374	0.59	21.6	0.000130	0.22	25.012	0.495	0.0530	0.0007	0.0399	0.0008	-	-	-	-	-	252	5	-	-	-

Notes: **1.** Uncertainties given at the one σ level; **2.** Error in FC1 reference zircon calibration was 0.38% & 0.72% for the analytical sessions (not included in above errors but required when comparing $^{206}Pb/^{238}U$ data from different mounts); **3.** f_{206}% denotes the percentage of ^{206}Pb that is common Pb; **4.** For areas older than ~800 Ma correction for common Pb made using the measured $^{204}Pb/^{206}Pb$ ratio; **5.** For areas younger than ~800 Ma correction for common Pb made using the measured $^{238}U/^{206}Pb$ and $^{207}Pb/^{206}Pb$ ratios following Tera and Wasserburg (1972) as outlined in Williams (1998); **6.** For % Disc, 0% denotes a concordant analysis.

TABLE 3. ANALYTICAL DATA FOR SAMPLE FO04-22 (SUMMARY OF SHRIMP U-Pb ZIRCON RESULTS FOR SAMPLE FO04-22).

							Total Ratios				Radiogenic Ratios							Age (Ma)				
Grain. spot	U (ppm)	Th (ppm)	Th/U	$^{206}Pb^*$ (ppm)	$^{204}Pb/^{206}Pb$	f_{206} %	$^{238}U/^{206}Pb$	±	$^{207}Pb/^{206}Pb$	±	$^{206}Pb/^{235}U$	±	$^{207}Pb/^{235}U$	±	$^{207}Pb/^{206}Pb$	±	ρ	$^{206}Pb/^{238}U$	±	$^{207}Pb/^{206}Pb$	±	% Disc
1.1	83	66	0.80	5.0	-	<0.01	14.427	0.224	0.0552	0.0017	0.0693	0.0011	-	-	-	-	-	432	7	-	-	-
2.1	304	131	0.43	10.9	0.000063	0.14	23.866	0.303	0.0527	0.0010	0.0418	0.0005	-	-	-	-	-	264	3	-	-	-
3.1	226	106	0.47	9.7	-	0.17	19.939	0.361	0.0540	0.0011	0.0501	0.0009	-	-	-	-	-	315	6	-	-	-
4.1	89	48	0.54	14.1	-	<0.01	5.442	0.075	0.0743	0.0019	0.1840	0.0026	1,906	0.059	0.0752	0.0021	0.448	1,089	14	1,073	56	-1
5.1	440	178	0.40	28.5	-	<0.01	13.261	0.159	0.0564	0.0007	0.0754	0.0009	-	-	-	-	-	469	6	-	-	-
7.1	477	156	0.33	20.0	0.000109	0.13	20.488	0.251	0.0536	0.0008	0.0487	0.0006	-	-	-	-	-	307	4	-	-	-
8.1	413	347	0.84	22.6	-	0.10	15.693	0.190	0.0555	0.0007	0.0637	0.0008	-	-	-	-	-	398	5	-	-	-
9.1	289	146	0.50	11.0	-	0.04	22.522	0.288	0.0522	0.0010	0.0444	0.0006	-	-	-	-	-	280	4	-	-	-
10.1	317	91	0.29	12.4	-	0.05	21.915	0.278	0.0525	0.0018	0.0456	0.0006	-	-	-	-	-	287	4	-	-	-
11.1	241	150	0.62	17.6	0.000037	<0.01	11.728	0.147	0.0570	0.0008	0.0854	0.0011	-	-	-	-	-	528	6	-	-	-
12.1	407	127	0.31	21.1	-	0.03	16.590	0.203	0.0544	0.0009	0.0603	0.0007	-	-	-	-	-	377	5	-	-	-
13.1	205	125	0.61	8.0	0.000141	0.13	22.190	0.297	0.0530	0.0012	0.0450	0.0006	-	-	-	-	-	284	4	-	-	-
14.1	251	86	0.34	26.9	0.000063	<0.01	8.033	0.100	0.0642	0.0008	0.1245	0.0016	-	-	-	-	-	757	9	-	-	-
15.1	327	199	0.61	11.6	-	0.10	24.174	0.308	0.0522	0.0010	0.0413	0.0005	-	-	-	-	-	261	3	-	-	-
16.1	152	149	0.98	7.4	0.000019	0.20	17.709	0.246	0.0552	0.0013	0.0564	0.0008	-	-	-	-	-	353	5	-	-	-
17.1	52	23	0.45	17.1	-	<0.01	2.613	0.040	0.1280	0.0014	0.3827	0.0058	6,756	0.128	0.1280	0.0014	0.808	2,089	27	2,071	20	-1
18.1	652	269	0.41	26.3	-	<0.01	21.297	0.255	0.0511	0.0007	0.0470	0.0006	-	-	-	-	-	296	3	-	-	-
19.1	1,078	651	0.60	204.7	0.000002	<0.01	4.525	0.052	0.0879	0.0003	0.2210	0.0025	2,678	0.032	0.0879	0.0003	0.947	1,287	13	1,380	7	7
20.1	110	49	0.44	5.6	-	0.23	16.726	0.250	0.0559	0.0015	0.0596	0.0009	-	-	-	-	-	373	6	-	-	-
21.1	280	107	0.38	11.5	-	<0.01	20.909	0.287	0.0517	0.0010	0.0479	0.0007	-	-	-	-	-	301	4	-	-	-
22.1	255	166	0.65	10.1	-	<0.01	21.588	0.284	0.0516	0.0011	0.0464	0.0006	-	-	-	-	-	292	4	-	-	-
23.1	642	189	0.29	35.8	0.000019	0.04	15.404	0.183	0.0552	0.0006	0.0649	0.0008	-	-	-	-	-	405	5	-	-	-
24.1	330	77	0.23	29.7	0.000067	0.03	9.547	0.117	0.0613	0.0007	0.1047	0.0013	-	-	-	-	-	642	8	-	-	-
25.1	198	281	1.42	9.9	0.000236	0.07	17.240	0.250	0.0544	0.0012	0.0580	0.0009	-	-	-	-	-	363	5	-	-	-
26.1	342	133	0.39	13.7	-	<0.01	21.483	0.273	0.0516	0.0011	0.0466	0.0006	-	-	-	-	-	293	4	-	-	-

Table 3 continued.

							Total Ratios				Radiogenic Ratios							Age (Ma)				
Grain. spot	U (ppm)	Th (ppm)	Th/U	$^{206}Pb^*$ (ppm)	$^{204}Pb/^{206}Pb$	f_{206} %	$^{238}U/^{206}Pb$	±	$^{207}Pb/^{206}Pb$	±	$^{206}Pb/^{238}U$	±	$^{207}Pb/^{235}U$	±	$^{207}Pb/^{206}Pb$	±	ρ	$^{206}Pb/^{238}U$	±	$^{207}Pb/^{206}Pb$	±	% Disc
27.1	406	91	0.22	22.7	0.000046	0.02	15.337	0.186	0.0550	0.0014	0.0652	0.0008	-	-	-	-	-	407	5	-	-	-
28.1	195	98	0.50	7.8	0.000187	<0.01	21.495	0.295	0.0509	0.0012	0.0466	0.0006	-	-	-	-	-	294	4	-	-	-
29.1	96	55	0.57	3.9	-	<0.01	21.389	0.341	0.0521	0.0018	0.0468	0.0008	-	-	-	-	-	295	5	-	-	-
30.1	639	450	0.70	24.9	0.000019	0.05	22.066	0.265	0.0524	0.0007	0.0453	0.0005	-	-	-	-	-	286	3	-	-	-
31.1	163	35	0.21	12.1	-	0.17	11.523	0.207	0.0595	0.0011	0.0866	0.0016	-	-	-	-	-	536	9	-	-	-
32.1	262	282	1.08	20.1	0.000066	0.03	11.174	0.141	0.0589	0.0009	0.0895	0.0012	-	-	-	-	-	552	7	-	-	-
33.1	161	115	0.71	6.5	0.000183	0.19	21.340	0.311	0.0537	0.0016	0.0468	0.0007	-	-	-	-	-	295	4	-	-	-
34.1	341	152	0.45	15.3	-	<0.01	19.186	0.247	0.0526	0.0011	0.0521	0.0007	-	-	-	-	-	328	4	-	-	-
35.1	161	104	0.64	6.9	0.000148	-0.14	20.105	0.298	0.0515	0.0015	0.0498	0.0007	-	-	-	-	-	313	5	-	-	-
36.1	404	248	0.61	16.0	-	<0.01	21.699	0.275	0.0515	0.0009	0.0461	0.0006	-	-	-	-	-	291	4	-	-	-
37.1	405	170	0.42	15.6	-	0.10	22.272	0.277	0.0528	0.0009	0.0449	0.0006	-	-	-	-	-	283	3	-	-	-
38.1	173	114	0.66	8.9	0.000065	<0.01	16.631	0.226	0.0531	0.0011	0.0602	0.0008	-	-	-	-	-	377	5	-	-	-
39.1	172	59	0.34	6.8	-	0.05	21.824	0.305	0.0525	0.0013	0.0458	0.0006	-	-	-	-	-	289	4	-	-	-
40.1	196	146	0.74	8.0	0.000090	<0.01	20.915	0.294	0.0517	0.0013	0.0479	0.0007	-	-	-	-	-	301	4	-	-	-
41.1	151	80	0.53	5.9	0.000236	<0.01	22.004	0.318	0.0516	0.0014	0.0455	0.0007	-	-	-	-	-	287	4	-	-	-
42.1	102	72	0.70	17.9	0.000009	0.02	4.903	0.072	0.0851	0.0011	0.2039	0.0030	2,389	0.046	0.0850	0.0011	0.761	1,196	16	1,315	24	9
43.1	25	9	0.35	1.0	0.001193	<0.01	21.965	0.539	0.0502	0.0033	0.0456	0.0011	-	-	-	-	-	288	7	-	-	-

Notes: **1.** Uncertainties given at the one σ level; **2.** Error in FC1 reference zircon calibration was 0.72% for the analytical sessions (not included in above errors but required when comparing $^{206}Pb/^{238}U$ data from different mounts); **3.** f_{206} % denotes the percentage of ^{206}Pb that is common Pb; **4.** For areas older than ~800 Ma correction for common Pb made using the measured $^{204}Pb/^{206}Pb$ ratio; **5.** For areas younger than ~800 Ma correction for common Pb made using the measured $^{238}U/^{206}Pb$ and $^{207}Pb/^{206}Pb$ ratios following Tera and Wasserburg (1972) as outlined in Williams (1998); **6.** For % Disc, 0% denotes a concordant analysis.

4. Results

4.1. Palynology

The palynological analysis revealed a palynoflora composed predominantly by Gymnospermopsida monosaccate pollen grains, although Gymnospermopsida bisaccate pollen grains were also observed. Selected species are illustrated in figure 3. The samples show a very low frequency of palynomorphs, and in most cases an exact identification of the species is impossible because of the bad preservation state of the palynomorphs. The palynomorphs detected within the TL are *Punctatisporites punctatus* (Ibrahim) Ibrahim, a Pteridophyta known from the Carboniferous to Triassic in New Zealand, Australia, Asia, Europe and South America (Alpern and Doubinger, 1973; Owens *et al.*, 2002; Pérez Loinaze, 2008).

The palynological association observed in the metasediments of the DYC (sampled in the Madre de Dios Archipelago and in the Diego de Almagro Island) is characterized by Gymnospermopsida pollen. In addition, Pteridophyta spores as well as rare green algae (*Botryococcus braunii* Kützing, Lower Carboniferous to Recent) and epiphyllous fungal spores (*Granatisporites* and *Multicellaesporites* spp.) have been observed. The Gymnospermopsida include Coniferales and Cordaitales. The more frequent monosaccate pollens are *Plicatipollenites* and *Cannanoropollis* spp., which are also represented in the Carboniferous-Permian of Gondwana (*e.g.*, Vergel, 2008; Di Pasquo, 2009). The bisaccate pollen grains of Gymnospermopsida are assigned to the *Protohaploxypinus* sp., also known in middle Carboniferous successions of Argentina, but recognized also in the Permian of Brazil, South Africa, India, Antarctica, Australia and North America (Césari and Gutiérrez, 2000, and reference therein). Remnants of polyplicate and monocolpate pollen grains, of 80-95 µm, assigned to *Praecolpatites sinuosus* (Balme and Hennelly) Bharadwaj and Srivastava, have been observed (sample FO04-22, Fig. 4). They have broad distribution in the Permian of Argentina, Brazil, Australia, Africa, Antarctica and New Zealand (*e.g.*, Lindström, 1995). Therefore, a Permian age for the deposition of the sediments of the DYC is inferred.

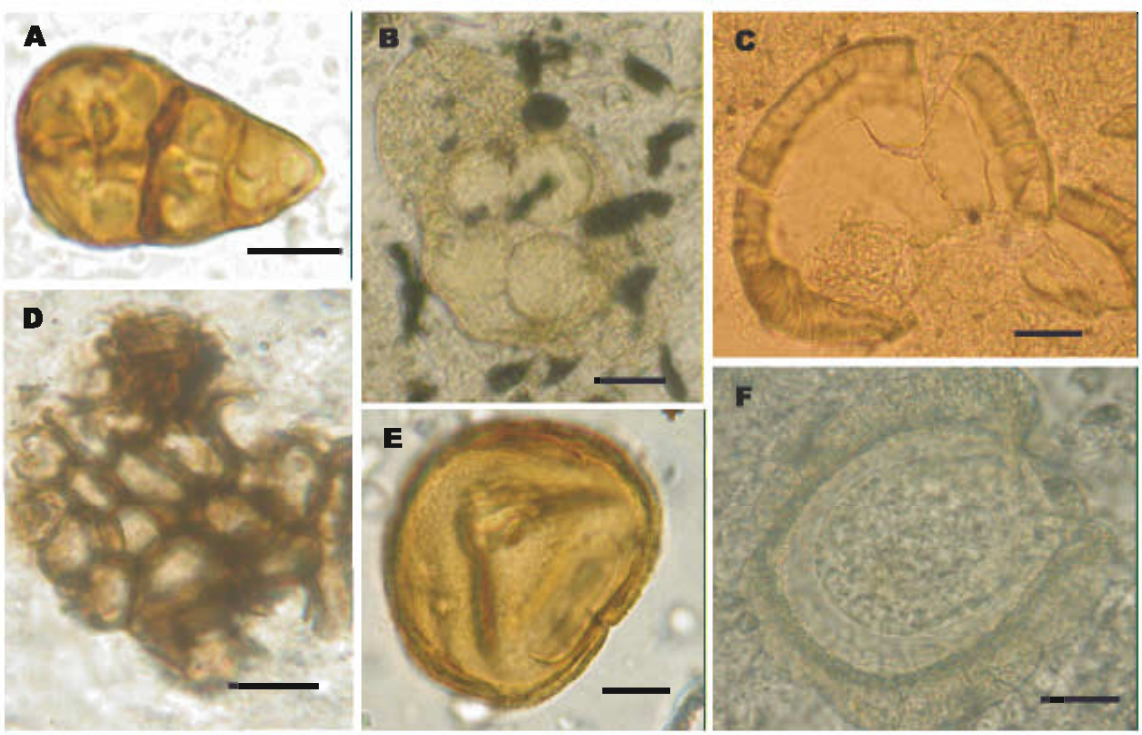

FIG. 3. Selected pollen grains, spores and algae from the studied samples. Black line represents 10 µm. **A.** *Granatisporites* sp.; **B.** *Protohaploxypinus* sp.; **C.** *Cannanoropollis* sp.; **D.** *Botryococcus braunii*; **E.** *Punctatisporites punctatus*; **F.** *Plicatipollenites* sp.

In addition, a humid environment of conifer and/or cordaitales forests with an undergrowth of ferns (probably developed on wet shaded slopes) is proposed from the palynological association recorded in the DYC.

4.2. Petrography

The metasedimentary samples collected for U-Pb zircon dating were obtained from an outcrop where the DC and the DYC are in conformable and intercalated stratigraphic contact (Fig. 4). Significantly, this site corresponds to one of only two localities were this type of contact between these complexes is recorded. The samples were spatially associated, stratigraphically separated by *ca.* 10 m. The first sample (FO04-21) comes from a deformed (folded) metasedimentary horizon (0.04 to 0.06 m thick) of tuffaceous character, interbedded in metacherts of the DC. The microscopic petrographic description of this sample shows that it is mainly composed by very angular fragments (0.01-0.2 mm) of quartz (55%), altered feldspars (30%) and biotite flakes (15%) in a cryptocrystalline siliceous matrix. Accessory minerals include zircon, garnet, sphene, apatite and Fe-oxides. Scarce small and highly altered shard fragments were also observed. The biotites are oriented parallel to the contacts with the underlying radiolarian chert. This last feature coupled with the normal grading observed in this bed agrees with subaquatic conditions of deposition. The second sample (FO04-22) is a quartz rich metasandstone of the DYC previously analyzed by palynological methods. The sample was extracted from a massive and structureless sandstone bed (20 m of minimum thickness) nearly 3 m above the contact with the banded cherts of the DC. It is a feldspathic arenite formed by well to moderately sorted subangular and highly spherical fragments, with sizes between 0.02 and 1.2 mm (0.3 mm in average). Main fragments are quartz (60%), feldspars (30%), biotite (8%) and white mica (2%). Accessories include zircon, apatite, lithic fragments (basalts and rhyolites), garnet, pyrite and Fe-oxides.

4.3. U-Pb SHRIMP ages of detrital zircons

The Tera-Wasserburg diagrams plot the total ratios, uncorrected for common Pb, and show that the data generally plot close to Concordia (Fig. 5). Relative probability spectra of the detrital zircon ages are presented in figure 5. For sample FO04-21 54 grains were analyzed, whereas 42 grains were examined for sample FO04-22.

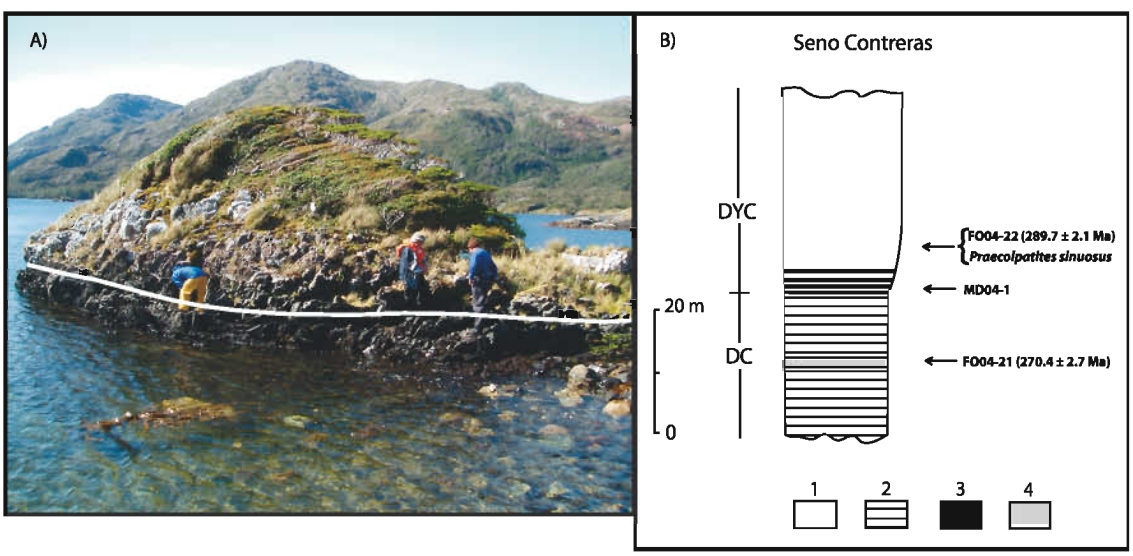

FIG. 4. **A.** Outcrops at Seno Contreras, where the stratigraphical contact between deformed banded cherts of the DC (above the white line) and shales and sandstones of the DYC (below) is observed; **B.** Stratigraphic column showing the disposition of the samples analyzed by U-Pb SHRIMP and by palynological methods. **1.** Sandstones; **2.** Banded cherts; **3.** Shales; **4.** Tuffaceous layer.

FO04-21. The zircons of this sample are prismatic and euhedral crystals, with zoned magmatic internal structures as seen under CL imaging (Fig. 6). This is compatible with its textural and mineralogical characteristics, which are indicative of the tuffaceous character of the metasediment. Although some of the youngest individual ages involve significant common Pb correction (Fig. 5); a correction has been applied to derive the radiogenic ratios and age of these analyses (Table 2). The age spectrum shows a narrow range of provenance ages with a major peak in the early middle Permian, representing *ca.* 76% of the analyses. Minor peaks are observed in the Carboniferous, Devonian, Ordovician, Cambrian and Neoproterozoic, each one equivalent to less than 8% of the total analyzed grains. The Permian analyses yield a weighted mean $^{206}Pb/^{238}U$ age of 270.4±2.7 Ma (MSWD=1.2), interpreted as the maximum possible depositional age of the analyzed metasediment.

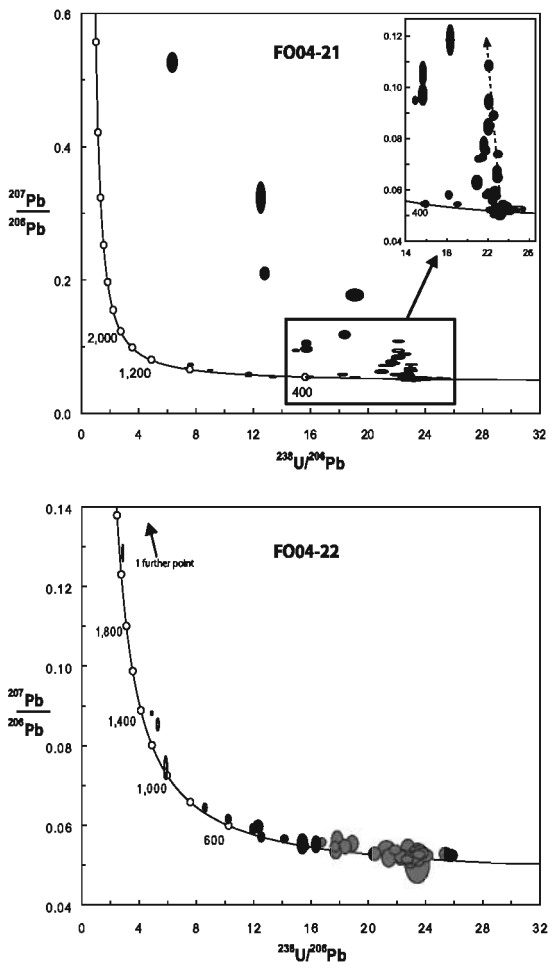

FIG. 5. Tera-Wasseburg diagrams for zircon U-Pb data. Analyses are plotted as total ratios calibrated for U-Pb, but uncorrected for common Pb. The error ellipses are 68.3% confidence limits. The dotted arrow in FO04-21 shows the direction of common Pb at 270 Ma. Alignment along this arrow suggests a real inferred age on Concordia with variable degrees of incorporated common Pb at the time of crystallization.

FO04-22. The zircon grains show zoned internal structures (Fig. 6), and subrounded to subangular shapes with high sphericity are predominant, although prismatic grains are observed as well. The grains analyzed from this sample are very low in common Pb. The relative probability plots of the detrital zircon ages display a prominent component in the early Permian (*ca.* 40% of the analyses), with other subordinate peaks in the Carboniferous and Devonian (*ca.* 17% of the analyses each one). There are scattered older ages ranging from Early Paleozoic to Neo and Mesoproterozoic aged noise and one Paleoproterozoic aged zircon. A weighted mean $^{206}Pb/^{238}U$ age of 289.7±2.1 Ma (MSWD=1.3) place a constraint on the maximum age of deposition of this metasediment.

5. Discussion

5.1. Regional paleoenvironmental conditions

As pointed out by Cúneo (1996) and Buatois *et al.* (2006), it seems that the end of the late Paleozoic Ice Age in Gondwana is diachronous, waning first in South America, as revealed by litho- and biostratigraphic records (*ca.* 280 Ma; Iannuzzi *et al.*, 2007), and then in Australia (*ca.* 260 Ma; Fielding *et al.*, 2008). This diachronism has been habitually attributed to the Gondwana drift across the South Pole (López-Gamundí *et al.*, 1994; Visser, 1996), but the possibility of more than one glacial event cannot be ruled out (Limarino *et al.*, 2006). Roscher and Schneider (2006) show that there is a general trend of aridization in the Permo-Carboniferous interrupted by wet phases related to the waxing and waning of the Gondwana icecap. Lindström and McLoughlin (2007) indicate that during the middle to late Permian a gradual warming trend is evident from the western to the eastern parts of Gondwana. Furthermore, semiarid and arid climatic conditions in middle Permian times appear like a common feature in many western Gondwana basins (López-Gamundí *et al.*, 1992; Limarino *et al.*, 2006; Spalletti

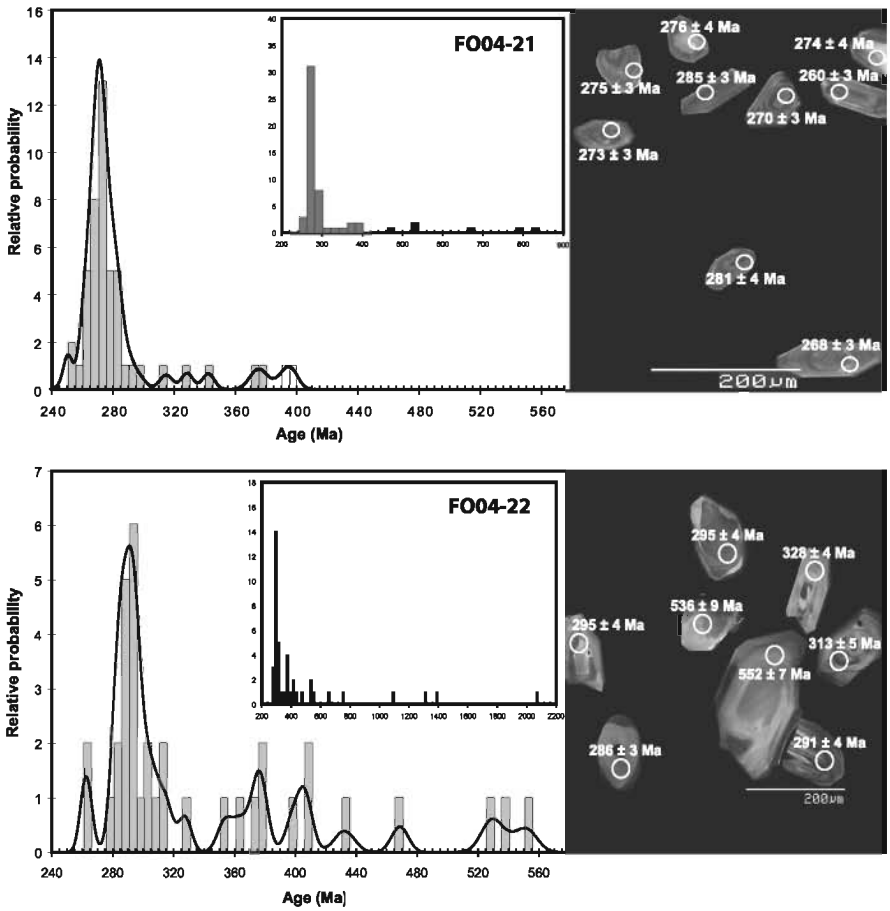

FIG. 6. U-Pb zircon age provenance patterns (age *versus* relative probability) of the analyzed samples. Insets show the entire population of zircon ages. Montages of representative portions of the cathode-luminescence images for each sample, with individual spot ages.

and Limarino, 2006; Souza *et al.*, 2007), while the start of arid conditions in western Gondwana has been situated towards the end of the early Permian by Césari *et al.* (2007).

Palynomorphs documented in this study are comparable to those recorded in Carboniferous and Permian strata of other late Paleozoic Gondwanan basins, such as those exposed in the Chaco-Paraná Basin in Argentina and Uruguay (Césari *et al.*, 1995; Beri *et al.*, 2006), and at Rio Grande do Sul in Paraná Basin, Brazil (Souza and Marques-Toigo, 2005). It is noteworthy to emphasize that the only palynomorph with exclusive Permian record (*Praecolpatites sinuosus*) is in one of the samples with a Permian maximum depositional age (Fig. 4). Regarding the paleoenvironmental background mentioned above and the Permian age obtained in the DYC, the proposed paleoclimatic setting for the deposition of the late Paleozoic basins of southwestern Gondwana, in particular those situated in Patagonia, helps to establish regional correlations and some paleoclimatic inferences. Archangelsky *et al.* (1996) and Limarino *et al.* (1996) suggested a specially humid and temperate climate, even subtropical, for the deposition of the La Golondrina Formation (the lower member in the La Golondrina Basin, Patagonia), whose age would be restricted between the Sakmarian and the Kungurian (Limarino and Spalletti, 2006). The age and paleoclimatic features of this formation are remarkable, particularly because it crops out in a relatively close position (*ca.* 500 km apart) to the present-day position of the outcrops of the DYC (Fig. 7). Another late Paleozoic Patagonian basin that shares similar paleoclimatic characteristics and also an adjacent location to the deposits of the DYC is the Tepuel-Genoa Basin (López-Gamundí and Limarino, 1984; Andreis *et al.*, 1987) (Fig. 7), likely related to metamorphic rocks outcropping in the Coastal Range of Chile (Hervé, 1988; Duhart *et al.*, 2001). The early Permian component of

this basin (Sakmarian-Artinskian, according to César *et al.*, 2007) is represented by the Río Genoa Formation, whose sediments have also been interpreted as deposited in a humid and subtropical climate (Archangelsky *et al.*, 1996; Limarino *et al.*, 1996). However, it is not possible to determine a more precise paleoclimatic connection with the La Golondrina Formation, mostly because late early Permian (Kungurian) sedimentary rocks have not been identified in the Tepuel-Genoa Basin (Limarino and Spalletti, 2006). If it is assumed a fixed position of the DYC with respect to Patagonia since its deposition, and considering the previous examples and the age obtained for the DYC, it would be probable that warm paleoclimatic conditions were recorded in the metasediments of this complex. This was, however, impossible to register in this study, mainly due to the very low proportion of palynological material in the samples.

Even though we cannot precise the paleoclimatic conditions during the deposition of the DYC, some observations can be done. The types of deposits accumulated as a consequence of ice activity are very varied, and several non-glacially related mechanisms can produce similar deposits. The recognition of these accumulations is more difficult if we consider that glacial deposits are frequently reworked in outwashes or by mass flow. For these reasons, the assignment of a glacial origin to any deposit, or its refutation, needs the combination of the properties of the deposit itself, the adjacent rocks units, as well as climatic and paleogeographic conditions at the time of deposition (*e.g.*, Charrier, 1986). Additionally, to establish that a sedimentary succession, or part of it,

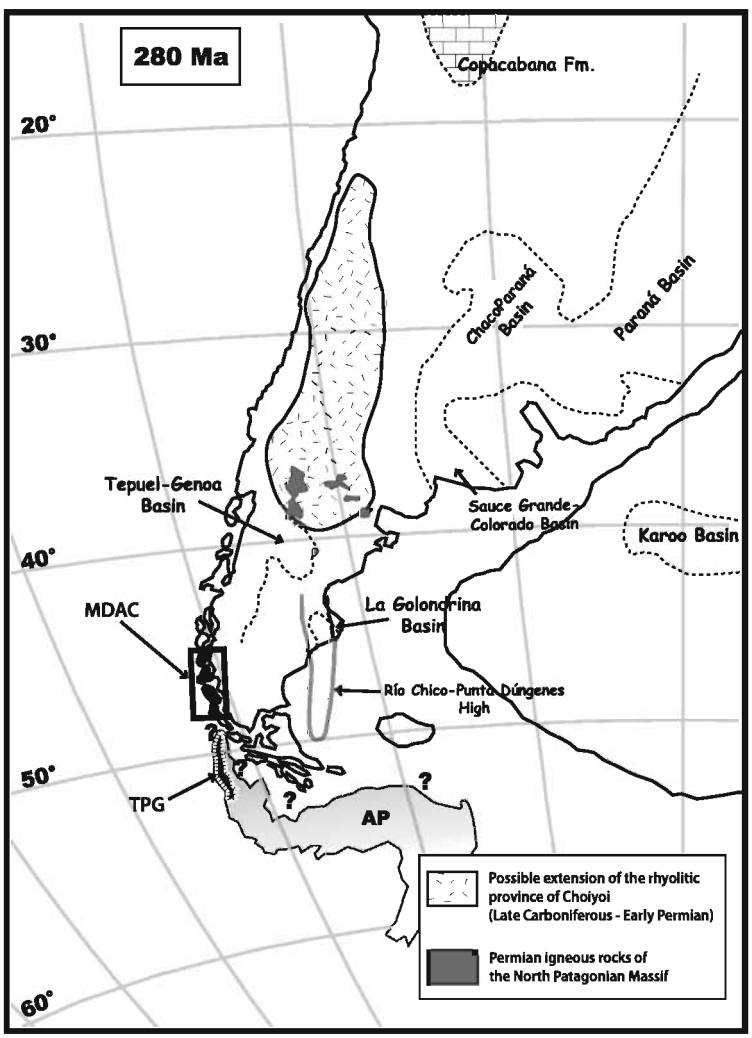

FIG. 7. Paleogeographic reconstruction for South America in the early Permian, based on the pole of Rapalini *et al.* (2006). Positions of the late Paleozoic basins (from Limarino and Spalletti, 2006), Choiyoi deposits (modified from Kay *et al.*, 1989; Ramos, 2000), and the current location of the outcrops of the Madre de Dios Accretionary Complex (MDAC) and the Trinity Peninsula Group (TPG) are shown, as well as the probable position of the Antarctic Peninsula (AP). The southern extension of the Río Chico-Punta Dúngenes high is taken from Ramos (2008), and the distribution of Permian igneous rocks of the North Patagonian Massif is from Pankhurst *et al.* (2006).

preserves a record of glacial, proglacial or periglacial depositional environments, multiple facies criteria are needed (diamictites, chaotic fabrics, rhythmites, laminated mudrocks with outsized dispersed clasts (lonestones), striated pavement, and faceted, bullet-shaped and striated clasts, among others; Miller, 1996), or it is required a single criterion that unambiguously appears to indicate glacial influence by virtue of its occurrence out of context with enclosing facies (*e.g.*, Fielding *et al.*, 2008). In this context, even though there have been records of diamictites in the DYC (Cecioni, 1956; Forsythe and Mpodozis, 1983), this does not give conclusive evidence of a glacial environment of deposition. Moreover, there are only few localities in the whole extension of this accretionary complex (more than 1,000 km^2) where diamictites have been identified, but the existence of glacial characteristics *sensu stricto* like lonestones (dropstones), striated pavements or faceted clasts have never been reported.

The large extension and volume of the DYC could be attributed to the great volume of fresh water produced by ice-melting during the waning of the glaciation in Gondwana (Buatois *et al.*, 2006). This huge volume of water probably reworked large amounts of sediments that were subsequently deposited at the margins of the continent. The ichnofaunas registered in DYC (*Scalarituba* isp., *Chondrites* isp., *Planolites* isp., *Palaeophycus* isp. and *Ancorichnus* isp.; *in* Lacassie, 2003), are distinctive of marine environments (written communication, L. Buatois, January 2008), and the low content of palynological material in the samples suggests a marine offshore environment of deposition of the host rocks. Both proposals match with the interpretation of the DYC rocks as turbidites, and would exclude a fjord-like setting for the origin of this succession and indicate that the place of deposition of the DYC was located far away from the direct influence of fresh water formed during the Gondwanan deglaciation.

5.2. Age and sources of metasediments

The detrital zircon data for sample FO04-21 of the DC reveal a maximum possible depositional age of this tuff-rich sediment of 270.4±2.7 Ma, roughly in the limit between the early Permian (Kungurian) and the middle Permian (Roadian). This result is identical to the youngest predominant detrital zircon U-Pb SHRIMP age component previously reported for samples of the DYC (*ca.* 270 Ma, Hervé *et al.*, 2003; Hervé *et al.*, 2006), and suggests that this peak is probably linked to a significant contribution of volcanic (tuffaceous) material deposited near the continental margin. This is also in agreement with the age of widespread ash fall deposits and tuffaceous horizons present in basins of the west Gondwana (Turner, 1999; Stollhofen *et al.*, 2000; López-Gamundí, 2006; Santos *et al.*, 2006, Tohver *et al.*, 2007), commonly correlated with the peak of the Choiyoi silicic volcanism during the late early Permian and middle Permian along the Andean Cordillera and its equivalents in Patagonia (López-Gamundí, 2006).

The data obtained for sample FO04-22 of the DYC (289.7±2.1 Ma) indicate an early Permian (Sakmarian) maximum possible depositional age. This is nearly 20 m.y. older than the youngest U-Pb SHRIMP ages component recorded for detrital zircons in the DYC (Hervé *et al.*, 2003). Nonetheless, the former authors have recognized this Sakmarian peak (*ca.* 290 Ma) as an individual Permian population in the age spectrum of the detrital zircons in the DYC. The apparent inverted stratigraphical position of the analyzed samples (Fig. 4) can be explained as FO04-21 being the airborne volcanic material deposited near the continental margin of Gondwana, and FO04-22 as resedimented detritus, formerly deposited somewhere between its local source area and the final depositional site, and then redeposited as turbidite flows above the cherts which include the tuffaceous layer represented by FO04-21.

Augustsson *et al.* (2006) suggest that the Permian sediments present in the metasedimentary complexes of Patagonia were probably largely supplied from local Patagonian and West Antarctic sources. Furthermore, Pankhurst *et al.* (2006) claim that the Permo-Triassic granites present in the North Patagonian Massif (extending between 41° and 44°S, approximately) can be identified as the most important source so far recognized for the provenance of detritus in the late Paleozoic metasedimentary rocks along the Pacific margin of Gondwana. This would imply transport by a system of long rivers over a wide and relatively flat pre-Andean platform (Hervé *et al.*, 2003), or even eolian transport over hundreds of kilometers (*e.g.*, Dickinson and Gehrels, 2009).

The widespread abundance of radiometric data from ash fall deposits within the range of 280 to 260 Ma has been commonly attributed to a period of intense silicic volcanism along the continental margin of southwestern Gondwana that peaked

around the 270 Ma (López-Gamundí, 2006). Besides the model of Pankhurst *et al.* (2006), until now no analogous magmatic process responsible for the ubiquitous Sakmarian peak (*ca.* 290 Ma) in the U-Pb spectrum from samples of the DYC has been clearly identified. Similar and equivalent radiometric ages have been obtained from adjacent late Paleozoic basins of southwestern Gondwana. In the southernmost Karoo Basin of South Africa, Bangert *et al.* (1999) reported 288.0±3.0 and 289.6±3.8 Ma from bentonitic tuff beds intercalated in sedimentary rocks of the Prince Albert Formation, lower Ecca Group. Rocha-Campos *et al.* (2006) and Guerra-Sommer *et al.* (2008) acquired comparable Permian ages from ash-fall deposits interbedded in coal successions of the southern Paraná Basin in Brazil. The last authors claim that this information supports the presence of an active and extensive volcanic event in western Gondwana around the Carboniferous-Permian boundary (*ca.* 299 Ma). It is, however, difficult to restrict the magmatic activity in southwestern Gondwana to a single instant in Permian times, since most of the limited available data are in the range of 270 to 290 Ma and usually they overlap within their analytical uncertainty. Instead, the entire early Permian could be regarded as a period of active and geographically widespread magmatism in this region of Gondwana. This scenario would also explain the strong coincidence of the main Permian peaks in the detrital zircon U-Pb spectrum of the metasediments of the DYC, the Rakaia Terrane (New Zealand) and the eastern Le May Group (Alexander Island, Antarctica) (Lacassie *et al.*, 2006). Nevertheless, the cause of the petrographic and geochemical similarities between these three metasedimentary units is an issue not discussed here as it is beyond the scope of this work.

5.3. Paleogeographic correlations

So far, there has been no consensus in the place of accretion of the TL and DC and the supposed subsequent sense of movement of the MDAC (as a coherent block) along the southwestern Gondwana margin. Lacassie *et al.* (2006) proposed accretion of the DC-TL assemblage at the Antarctic-Australian portion of the Gondwana margin, followed by dextral translation of the MDAC (and hence of the DYC) parallel to the margin. On the other hand, the possibility of a virtually fixed position for the DYC since its deposition (with Patagonia as reference) is hampered by the fact that there is no clear indication of a coeval Permian magmatic arc at latitude similar to the current position of the MDAC in southern Patagonia (*e.g.*, Hervé *et al.*, 2006). This magmatic arc could be represented either by the Choiyoi acid magmatic province (Kay *et al.*, 1989; Mpodozis and Kay, 1990) or by the Permian igneous rocks in the North Patagonian Massif (Pankhurst *et al.*, 2006), both sources currently located north of the 40° and 44°S, respectively. However, the Choiyoi Formation presents ages of *ca.* 281 Ma near its base (Rocha-Campos *et al.*, 2006; Suárez *et al.*, 2009), and thus cannot account for the 290 Ma peak in the U-Pb age spectrum. Conversely, it is well known that the subduction of bathymetrically elevated oceanic features such as ridges or plateau (DC and TL in this case) can flatten the subducting slab and prevent the magmatic activity in the vicinity of the continental margin. According to the above-mentioned situation, the DYC would not have had displacement since its deposition and the remnants of the associated Permian magmatic arc could still be hidden below the Mesozoic sedimentary cover somewhere in the southeastern Patagonia or even farther eastward. This option has been recently explored by Ramos (2008), who proposes a late Paleozoic magmatic arc with a southern extension in the NNE trending Río Chico-Punta Dúngenes High (Fig. 7). This hypothesis would preclude defining the DYC as an allochthonous terrane. A precedent that supports this hypothesis is the presence of metasedimentary rocks with detrital zircons with U-Pb SHRIMP ages similar (*ca.* 290 Ma) to the ones recorded in the DYC to the east of the South Patagonian Batholith, at almost the same latitude of the MDAC (Augustsson *et al.*, 2006). In brief, additional and more detailed paleomagnetic, geochronological and isotopic work is needed to give more convincing arguments supporting one of the proposed hypotheses, an autochthonous or an allochthonous origin of the DYC.

Little is known about the exact paleogeographic configuration of the Antarctic Peninsula during the late Paleozoic, though one of the most accepted current paleogeographic reconstructions locate the Antarctic Peninsula lying west of Patagonia in the Middle Jurassic (König and Jokat, 2006). Therefore, the possibility of a geological correlation between the geologic units present in western Patagonia and those exposed in the Antarctic Peninsula must be considered. In this context, it has been suggested based on the similarity of lithology and detrital zircon

age patterns, that the Trinity Peninsula Group (TPG) is the equivalent counterpart of the DYC in the Antarctic Peninsula (Hervé *et al.*, 2006) (Fig. 7). Willan (2003) assumed that the TPG could have been derived from a glaciated continental margin, though his result is based only on indirect evidence (geochemical weathering) and, at this time, there are no palynological reports on this unit. According to the paleogeographic reconstructions for the late Paleozoic (*e.g.*, Cawood and Buchan, 2007), the TPG was supposedly located in a higher paleolatitudinal position than the late Paleozoic Patagonian basins, and therefore the paleoclimatic conditions would have been colder during its deposition. However, caution must be taken with this interpretation, mainly because the TPG is part of the Western Domain of the Antarctic Peninsula (Vaughan and Storey, 2000), which has been regarded as a suspect terrane and even as allochthonous to the rest of the terranes of the Antarctic Peninsula (Willan, 2003).

6. Conclusions

This contribution presents the first palynological record for the late Paleozoic in Chile. The palynological assemblage recorded in the DYC is composed mainly of Gymnospermopsida pollen, with also Pteridophyta and fungal spores. The studied association indicates a humid environment of forests with an undergrowth of ferns.

The palynological data indicate a Permian age for the deposition of the DYC. This age is also supported by new U-Pb SHRIMP detrital zircon ages, which constrain the maximum depositional age of the DYC to the limit between the early Permian and the middle Permian (*ca.* 270 Ma), confirming the maximum depositional age obtained by previous geochronological data (Hervé *et al.*, 2003).

The available data indicate that the allochthonous hypothesis for the DYC is not completely proved, and an autochthonous tectonic setting (with respect to Patagonia) could also be a possible interpretation.

Acknowledgements

CONICYT doctoral grant to FAS, Fondecyt 1050431, Proyecto Anillo Antártico ARGT 04, Compañía de Aceros del Pacífico (CAP-Mina Guarello) and Expedición Última Patagonia 2006 supported this research. D. Quiroz (SERNAGEOMIN), A. Vidal and S. Martini are thanked for field support. We are indebted to Dr. C. Juliani (Universidade de São Paulo) for make possible sampling on Diego de Almagro Archipelago. Thanks also for Dr. A. Rapalini (Universidad de Buenos Aires) for his paleogeographic reconstructions. Drs. J.P. Lacassie and P. Vásquez contributed with fruitful discussions. We also thank C. Limarino (Universidad de Buenos Aires), H. Bahlburg (WWU Münster) and an anonymous referee for their helpful comments on an early version of this manuscript, as well as the careful editorial handling by M. Suárez.

References

Alpern, B.; Doubinger, J. 1973. Les miospores monolètes du Paléozoique. *In* Microfossiles organiques du Paléozoique 6: Les spores (Alpern, B.; Streel, M.; editors). Commission Internationale de Microflore du Paléozoique, Centre National de la Recherche Scientifique, Paris: 103 p.

Andersen, T. 2005. Detrital zircons as tracers of sedimentary provenance: limiting conditions from statistics and numerical simulation. Chemical Geology 216: 249-270.

Andreis, R.R.; Archangelsky, S.; González, C.R.; López-Gamundí, O.; Sabattini, N. 1987. Cuenca Tepuel-Genoa. *In* El Sistema Pérmico en la República Argentina y en la República Oriental del Uruguay (Archangelsky, S.; editor). Academia Nacional de Ciencias: 155-182. Córdoba.

Archangelsky, S.; Jalfin, G.; Cúneo, R. 1996. Cuenca La Golondrina. *In* El Sistema Pérmico en la República Argentina y en la República Oriental del Uruguay (Archangelsky, S.; editor). Academia Nacional de Ciencias: 93-108. Córdoba.

Augustsson, C.; Münker, C.; Bahlburg, H.; Fanning, C.M. 2006. Provenance of late Palaeozoic metasediments of the SW South American Gondwana margin: a combined U-Pb and Hf-isotope study of single detrital zircons. Journal of the Geological Society of London 163: 983-995.

Bangert, B.; Stollhofen, H.; Lorenz, V.; Armstrong, R.L. 1999. The geochronology and significance of ash-fall tuffs in the glacigenic, Carboniferous-Permian Dwyka Group of Namibia and South Africa. Journal of African Earth Sciences 29: 33-49.

Beri, A.; Gutiérrez, P.; Cernuschi, F.; Balarino, M.L. 2006. Palinología del Pérmico Inferior en la perforación DCLS-24 (Formación San Gregorio), departamento de Cerro Largo, Uruguay. Parte I: esporas, algas, prasinofitas y acritarcas. Ameghiniana 43 (1): 227-244.

Buatois, L.A.; Netto, R.G.; Mángano, M.G.; Balistieri, P.R.M.N. 2006. Extreme freshwater release during the

late Paleozoic Gondwana deglaciation and its impact on coastal ecosystems. Geology 34 (12): 1021-1024.

Cabrera La Rosa, A.; Petersen, G. 1936. Reconocimiento geológico de los yacimientos petrolíferos del departamento de Puno. Boletín del Cuerpo de Ingenieros de Minas del Perú 115: 1-100.

Cawood, P.A. 2005. Terra Australis Orogen: Rodinia breakup and development of the Pacific and Iapetus margins of Gondwana during the Neoproterozoic and Paleozoic. Earth-Science Reviews 69: 249-279.

Cawood, P.; Buchan, C. 2007. Linking accretionary orogenesis with supercontinent assembly. Earth-Science Reviews 82: 217-256.

Cawood, P.A.; Landis, C.A.; Nemchin, A.A.; Hada, S. 2002. Permian fragmentation, accretion and subsequent translation of a low-latitude Tethyan seamount to the high-latitude east Gondwana margin: evidence from detrital zircon age data. Geological Magazine 139: 131-144.

Cecioni, G. 1955. Noticias preliminares sobre la existencia del Paleozoico superior en el archipiélago patagónico entre los 50° y 52°S. Universidad de Chile, Instituto Geológico, Publicaciones 8: 181-202.

Cecioni, G. 1956. Primeras noticias sobre la existencia del Paleozoico Superior en el Archipiélago Patagónico entre los paralelos 50° y 52°S. Universidad de Chile, Facultad de Ciencias Físicas y Matemáticas, Anales 13: 183-202.

Césari, S.N.; Archangelsky, S.; Seoane, L. 1995. Palinología del Paleozoico Superior de la perforación Las Mochas, provincia de Santa Fe, Argentina. Ameghiniana 32: 73-106.

Césari, S.N.; Gutiérrez, P.R. 2000. Palynostratigraphy of Upper Paleozoic sequences in central-western Argentina. Palynology 24: 113-146.

Césari, S.N.; Gutiérrez, P.R.; Sabattini, N.; Archangelsky, A.; Azcuy, C.L.; Carrizo, H.A.; Cisterna, G.; Crisafully, A.; Cúneo, R.N.; Díaz Saravia, P.; Di Pasquo, M.; González, C.R.; Lech, R.; Pagani, M.A.; Sterren, A.; Taboada, A.C.; Vergel, M.M. 2007. Paleozoico Superior en Argentina: un registro fosilífero integral en el Gondwana occidental. Asociación Paleontológica Argentina. Ameghiniana 50° aniversario: 35-54. Buenos Aires.

Chamot, G.A. 1965. Permian section at Apillapampa, Bolivia, and its fossil content. Journal of Paleontology 39 (6): 1112-1124.

Charrier, R. 1986. The Gondwana Glaciation in Chile: description of alleged glacial deposits and palaeogeographic conditions bearing on the extension of the ice cover in southern South America. Palaeogeography, Palaeoclimatology, Palaeoecology 56: 151-175.

Cocks, L.R.M.; Torsvik, T.H. 2006. European geography in a global context from the Vendian to the end of the Palaeozoic. *In* European Lithosphere Dynamics (Gee, D.G.; Stephenson, R.A.; editors). Geological Society of London, Memoirs 32: 83-95.

Coney, P.J.; Jones, D.L.; Monger, J.W.H. 1980. Cordilleran suspect terranes. Nature 288: 329-333.

Coombs, D.S. 1997. A note on the terrane concept, based on a introduction to the Terrane '97 conference, Christchurch, New Zealand, February 1997. American Journal of Science 297: 762-764.

Cúneo, N.R. 1996. Permian phytogeography in Gondwana. Palaeogeography, Palaeoclimatology, Palaeoecology 125: 75-104.

Cunningham, W.D. 1993. Strike-slip faults in the southernmost Andes and the development of the Patagonian orocline. Tectonics 12: 169-186.

Dickinson, W.R.; Gehrels, G.E. 2009. U-Pb ages of detrital zircons in Jurassic eolian and associated sandstones of the Colorado Plateau: Evidence for transcontinental dispersal and intraregional recycling of sediment. Geological Society of America Bulletin 121: 408-433.

Di Pasquo, M. 2009. Primer registro de megafloras y palinología en estratos de la Formación Tarija (Pennsylvaniano), Arroyo Aguas Blancas, Provincia de Salta, Argentina: Descripción de dos especies nuevas. Andean Geology 36 (1): 95-123.

Douglass, R.C.; Nestell, M.K. 1972. Fusulinid foraminifera from southern Chile. Anais da Academia Brasileira de Ciências 44: 119-125.

Douglass, R.C.; Nestell, M.K. 1976. Late Paleozoic Foraminifera from southern Chile. United States Geological Survey, Professional Paper 858: 47 p.

Duhart, P.; McDonough, M.; Muñoz, J.; Martin, M.; Villeneuve, M. 2001. El Complejo metamórfico Bahía Mansa en la cordillera de la Costa del centro-sur de Chile (39°30'-42°00'S): geocronología K-Ar, $^{40}Ar/^{39}Ar$ y U-Pb e implicancias en la evolución del margen sur-occidental de Gondwana. Revista Geológica de Chile 28 (2): 179-208.

Duhart, P.; Muñoz, J.; Tassinari, C.; Quiroz, D. 2003. K-Ar Geochronology and Sr and Nd isotopic composition of the Patagonian Batholith in the Madre de Dios Archipelago (50°30'S), Southern Chile. *In* South American Symposium on Isotope Geology, No. 4, Short Papers: 542-544. Salvador de Bahía.

Faúndez, V.; Hervé, F.; Lacassie, J.P. 2002. Provenance and depositional setting of pre-Late Jurassic turbidite

complexes in Patagonia, Chile. New Zealand Journal of Geology and Geophysics 45: 411-425.

Fielding, C.R.; Frank, T.D.; Birgenheier, L.P.; Rygel, M.C.; Jones, A.T.; Roberts, J. 2008. Stratigraphic imprint of the Late Palaeozoic Ice Age in eastern Australia: a record of alternating glacial and nonglacial climate regime. Journal of the Geological Society of London 165: 129-140.

Forsythe, R. 1982. The late Palaeozoic to early Mesozoic evolution of southern South America: a plate tectonic interpretation. Journal of the Geological Society of London 139: 671-682.

Forsythe, R.D.; Mpodozis, C. 1979. El archipiélago de Madre de Dios, Patagonia Occidental, Magallanes: rasgos generales de la estratigrafía y estructura del basamento pre-Jurásico Superior. Revista Geológica de Chile 7: 13-29.

Forsythe, R.D.; Mpodozis, C. 1983. Geología del Basamento pre-Jurásico Superior en el Archipiélago Madre de Dios, Magallanes, Chile. Servicio Nacional de Geología y Minería, Boletín 39: 63 p.

Gradstein, F.M.; Ogg, J.G.; Smith, A. (editors) 2004. A Geological Time Scale 2004. Cambridge University Press: 589 p. Cambridge.

Guerra-Sommer, M.; Cazzulo-Klepzig, M.; Laquintinie, M.L.; Menegat, R.; Mendoça, J.G. 2008. U-Pb dating of tonstein layers from a coal succession of the southern Paraná Basin (Brazil): A new geochronological approach. Gondwana Research 14: 474-482.

Halpern, M. 1973. Regional Geochronology of Chile south of 50° latitude. Geological Society of America, Bulletin 84: 2407-2422.

Hervé, F.; Davidson, J.; Godoy, E.; Mpodozis, C.; Covacevich, V. 1981. The Late Paleozoic in Chile: Stratigraphy, structure and possible tectonic framework. Anais da Academia Brasileira de Ciências 53 (2): 362-373.

Hervé, F. 1988. Late Paleozoic subduction and accretion in Southern Chile. Episodes 11 (3): 183-188.

Hervé, F.; Fanning, M.; Bradshaw, J.; Bradshaw, M.; Lacassie, J.P. 1999. Late Permian SHRIMP U-Pb detrital zircon ages constrain the age of accretion of oceanic basalts to the Gondwana margin at the Madre de Dios Archipelago, southern Chile. *In* International Symposium on Andean Geodynamics, No. 4, Extended Abstracts Volume: 327-328. Göttingen.

Hervé, F.; Demant, A.; Ramos, V.; Pankhurst, R.J.; Suárez, M. 2000. The Southern Andes. *In* Tectonic evolution of South America (Cordani, U.G.; Milani, E.J.; Thomas Filho, A.; Campos, D.A.; editors). *In* International Geological Congress, No. 31: 605-634. Río de Janeiro.

Hervé, F.; Fanning, C.M.; Pankhurst, R.J. 2003. Detrital zircon age patterns and provenance of the metamorphic complexes of southern Chile. Journal of South American Earth Sciences 16: 107-123.

Hervé, F.; Mpodozis, C. 2005. The western Patagonia terrane collage: new facts and some thought-provoking possibilities. *In* Geological and Biological heritage of Gondwana (Pankhurst, R.J.; Veiga, G.D.; editors), Gondwana 12, Abstracts: p. 196. Mendoza.

Hervé, F.; Miller, H.; Pimpirev, C. 2006. Patagonia-Antarctica connections before Gondwana break-up. *In* Antarctica: Contributions to global earth sciences (Fütterer, D.K.; Damaske, D.; Kleinschmidt, G.; Miller, H.; Tessensohn, F.; editors). Springer-Verlag, Berlin Heidelberg: 217-228. New York.

Hervé, F.; Pankhurst, R.J.; Fanning, C.M.; Calderón, M.; Yaxley, G.M. 2007a. The South Patagonian batholith: 150 my of granite magmatism on a plate margin. Lithos 97: 373-394.

Hervé, F.; Faúndez, V.; Calderón, M.; Massonne, H-.J.; Willner, A.P. 2007b. Metamorphic and plutonic basement complexes. *In* The Geology of Chile (Moreno, T.; Gibbons, W.; editors). The Geological Society: 5-19. London.

Howell, D.G.; Jones, D.L.; Schermer, E.R. 1985. Tectonostratigraphic terranes of the Circum-Pacific region. *In* Tectonostratigraphic Terranes of the Circum-Pacific Region (Howell, D.G.; editor). Council for Energy and Mineral Resources, Earth Science Series 1: 3-30.

Hyden, G.; Tanner, P.W.G. 1981. Late Paleozoic-early Mesozoic fore-arc basin sedimentary rocks at the Pacific margin in western Gondwana. Geologische Rundschau 70: 529-541.

Iannuzzi, R.; Souza, P.A.; Holz, M. 2007. Lower Permian post-glacial succession in the southernmost Brazilian Paraná Basin: stratigraphy and floral (macro and micro) record. *In* European Meeting on the Palaeontology and Stratigraphy of Latin America, No. 4 (Díaz-Martínez, E.; Rábano, I; editors). Instituto Geológico y Minero de España, Cuadernos del Museo Geominero 8: 207-212. Madrid.

Isbell, J.L.; Lenaker, P.A.; Askin, R.A.; Miller, M.F.; Babcock, L.E. 2003. Reevaluation of the timing and extent of late Paleozoic glaciation in Gondwana: role of the Transantarctic Mountains. Geology 31 (11): 977-980.

Isbell, J.L.; Miller, M.F.; Lenaker, P.A.; Koch, Z.; Askin, R. 2005. How extensive was Gondwana glaciation in Antarctica? *In* Geological and Biological heritage of Gondwana (Pankhurst, R.J.; Veiga, G.D.; editors), Gondwana12, Abstracts: p. 205. Mendoza.

Kay, S.M.; Ramos, V.A.; Mpodozis, C.; Sruoga, P. 1989. Late Paleozoic to Jurassic silicic magmatism at the Gondwanaland margin: analogy to the Middle Proterozoic in North America? Geology 17: 324-328.

König, M.; Jokat, W. 2006. The Mesozoic breakup of the Wedell Sea. Journal of Geophysical Research 111, B12102, doi: 10.1029/2005JB00435.

Lacassie, J.P. 2003. Estudio de la proveniencia sedimentaria de los complejos metamórficos de los Andes Patagónicos (46°-51°S) mediante la aplicación de redes neuronales e isótopos estables. Doctoral Thesis (Unpublished), Universidad de Chile, Departamento de Geología: 204 p.

Lacassie, J.P.; Hervé, F.; Roser, B. 2006. Sedimentary provenance study of the post-Early Permian to pre-Early Cretaceous metasedimentary Duque de York Complex, Chile. Revista Geológica de Chile 33 (2): 199-219.

Limarino, C.O.; Andreis, R.R.; Ferrando, L. 1996. Paleoclimas del Paleozoico Tardío. *In* El Sistema Pérmico en la República Argentina y en la República Oriental del Uruguay (Archangelsky, S.; editor). Academia Nacional de Ciencias: 227-238. Córdoba.

Limarino, C.O.; Spalletti, L.A. 2006. Paleogeography of the upper Paleozoic basins of southern South America: An overview. Journal of South American Earth Sciences 22: 134-155.

Limarino, C.O.; Tripaldi, A.; Marenssi, S.; Fauqué; L. 2006. Tectonic, sea-level, and climatic controls on Late Paleozoic sedimentation in the western basins of Argentina. Journal of South American Earth Sciences 22: 205-226.

Lindström, S. 1995. Early Late Permian palynostratigraphy and palaeo-biogeography of Vestfjella, Dronning Maud Land, Antarctica. Review of Palaeobotany and Palynology 86: 157-173.

Lindström, S.; McLoughlin, S. 2007. Synchronous palynofloristic extinction and recovery after the end-Permian event in the Prince Charles Mountains, Antarctica: Implications for palynofloristic turnover across Gondwana. Review of Palaeobotany and Palynology 145: 89-122.

Ling, H.Y.; Forsythe, R.D.; Douglass, C.R. 1985. Late Paleozoic microfaunas from Southernmost Chile and their relation to Gondwanaland forearc development. Geology 13: 357-360.

Ling, H.Y.; Forsythe, R.D. 1987. Late Paleozoic pseudoalbaillellid radiolarians from southernmost Chile and their geological significance. *In* Gondwana Six: structure, tectonics, and geophysics (MacKenzie, G.D.; editor). Geophysical Monograph 40: 253-260. Washington, D.C.

López-Gamundí, O.; Limarino, C. 1984. Facies de abanico submarino en el Grupo Tepuel (Paleozoico superior), provincia del Chubut. Revista de la Asociación Geológica Argentina 39: 251-261.

López-Gamundí, O.R.; Limarino, C.; Césari, S. 1992. Late Paleozoic paleoclimatology of central west Argentina. Palaeogeography, Palaeoclimatology, Palaeoecology 91: 305-329.

López-Gamundí, O.R.; Espejo, I.S.; Conaghan, P.J.; Powell, C. 1994. Southern South America. *In* Permian-Triassic Pangea Basins and Foldbelts along the Panthalassan Margin of Gondwanaland (Veevers, J.; Powell, C.; editors). Geological Society of America, Memoir 184: 281-329.

López-Gamundí, O.R. 2005. Controls on pre-breakup (Carboniferous-Triassic) source rock distribution in southwestern Gondwanaland. *In* Geological and Biological heritage of Gondwana (Pankhurst, R.J.; Veiga, G.D.; editors), Gondwana 12, Abstracts: p. 234. Mendoza.

López-Gamundí, O.R. 2006. Permian plate margin volcanism and tuffs in adjacent basins of west Gondwana: Age constraints and common characteristics. Journal of South American Earth Sciences 22: 227-238.

Ludwig, K.R. 2001. SQUID 1.02: A User's Manual; Berkeley Geochronology Center Special Publication 2: 19 p.

Ludwig, K.R. 2003. Isoplot/Ex version 3.0: A geochronological toolkit for Microsoft Excel. Berkeley Geochronology Center Special Publication 4: 70 p.

Mamet, B. 1996. Late Paleozoic small foraminifers (endothyrids) from South America (Ecuador and Bolivia). Canadian Journal of Earth Sciences 33 (3): 452-459.

Miller, J.M.G. 1996. Glacial sediments. *In* Sedimentary environments: processes, facies, and stratigraphy (Reading, H.G.; editor). Blackwell Science: 454-483. Oxford.

Miller, H. 2007. History of views on the relative positions of Antarctica and South America: a 100-year tango between Patagonia and the Antarctic Peninsula. *In* Antarctica: A Keystone in a Changing World-Online Proceedings of the 10th ISAES (Cooper, A.K.; Raymond C.R.; *et al.*; editors). United States Geological Survey Open-File Report 2007-1047, Short Research Paper 041: 4 p.

Mpodozis, C.; Forsythe, R. 1983. Stratigraphy and geochemistry of accreted fragments of the ancestral Pacific floor in southern South America. Palaeogeography, Palaeoclimatology, Palaeoecology 41: 103-124.

Mpodozis, C.; Kay, S.M. 1990. Provincias magmáticas ácidas y evolución tectónica de Gondwana: Andes Chilenos (28-31°S). Revista Geológica de Chile 17: 153-180.

Olivares, B.; Cembrano, J.; Hervé, F.; López, G.; Prior, D. 2003. Geometría y cinemática de la zona de cizalle Seno Arcabuz, Andes Patagónicos, Chile. Revista Geológica de Chile 30 (1): 39-52.

Owens, B.; Zhu, H.; Turner, N. 2002. Comparative palynostratigraphy of the early Arnsbergian (Namurian) sequences between Great Britain and northwest China. Review of Palaeobotany and Palynology 118: 227-238.

Ozawa, T.; Kanmera, K. 1984. Tectonic terranes of Late Paleozoic rocks and their accretionary history in the circum-Pacific region viewed from Fusulinacean paleobiogeography. *In* Proceedings of the Circum-Pacific Terrane Conference (Howell, D.G.; Jones, D.L.; Cox, A.; Nur, A.; editors). Stanford University Press Publications 18: 158-160.

Paces, J.B.; Miller, J.D. 1993. Precise U-Pb ages of Duluth Complex and related mafic intrusions, northeastern Minnesota: Geochronological insights to physical, petrogenetic, paleomagnetic, and tectonomagmatic process associated with the 1.1 Ga Midcontinent Rift System. Journal of Geophysical Research 98: 13997-14013.

Pankhurst, R.J.; Rapela, C.W.; Fanning, C.M.; Márquez, M. 2006. Gondwanide continental collision and the origin of Patagonia. Earth-Science Reviews 76: 235-257.

Pérez Loinaze, V. 2008. Estudio sistemático palinológico de la Formación Cortaderas (Mississippiano), Cuenca Río Blanco, Argentina: Parte I. Ameghiniana 45 (1): 33-57.

Ramos, V.A. 1988. Late Proterozoic-Early Paleozoic of South America-a collisional history. Episodes 11 (3): 168-174.

Ramos, V.A. 2000. The southern central Andes. *In* Tectonic Evolution of South America (Cordani, U.; Milani, E.J.; Thomaz Filho, A.; Campos, D.A.; editors). *In* International Geological Congress, No. 31: 561-604. Río de Janeiro.

Ramos, V.A. 2008. Patagonia: A paleozoic continent adrift? Journal of South American Earth Sciences 26 (3): 235-251.

Rapalini, A.; Hervé, F.; Ramos, V.; Singer, S. 2001. Paleomagnetic evidence for a very large counterclockwise rotation of the Madre de Dios Archipelago, southern Chile. Earth and Planetary Science Letters 184: 471-487.

Rapalini, A.; Fazzito, S.; Orué, D. 2006. A new Late Permian paleomagnetic pole for stable South America: The Independencia group, eastern Paraguay. Earth Planets Space 58: 1247-1253.

Rocha-Campos, A.C.; Basei, M.A.S.; Nutman, A.P.; Santos, P.R. 2006. Shrimp U-Pb zircon geochronological calibration of the Late Paleozoic Supersequence, Parana Basin, Brazil. *In* South American Symposium on Isotope Geology, No. 5: 298-301. Punta del Este.

Rocha-Campos, A.C.; dos Santos, P.R.; Canuto, J.R. 2008. Late Paleozoic glacial deposits of Brazil: Paraná Basin. The Geological Society of America, Special Paper 441: 97-114.

Roscher, M.; Schneider, J.W. 2006. Permo-Carboniferous climate: Early Pennsylvanian to Late Permian climate development of central Europe in a regional and global context. *In* Non-Marine Permian Biostratigraphy and Biochronology (Lucas, S.G.; Cassinis, G.; Schneider, J.W.; editors). Geological Society, Special Publications 265: 95-136. London.

Sambridge, M.S.; Compston, W. 1994. Mixture modelling of multi-component data sets with application to ion-probe zircon ages. Earth and Planetary Science Letters 128: 373-390.

Santos, R.V.; Souza, P.A.; Souza de Alvarenga, C.J.; Dantas, E.L.; Pimentel, M.M.; de Oliveira, C.G.; de Araújo, L.M. 2006. SHRIMP U-Pb zircon dating and palynology of bentonitic layers from the Permian Irati Formation, Paraná Basin, Brazil. Gondwana Research 9: 456-463.

Sepúlveda, F. 2004. Metamorfismo de bajo grado en rocas del Complejo Denaro, archipiélago Madre de Dios, XII Región. Graduation Thesis (Unpublished), Universidad de Chile, Departamento de Geología: 49 p.

Sepúlveda, F.A.; Hervé, F.; Calderón, M.; Lacassie, J.P. 2008. Petrology of igneous and metamorphic units from the allochthonous Madre de Dios Terrane, Magallanes, Chile. Gondwana Research 13 (2): 238-249.

Souza, P.A.; Marques-Toigo, M. 2005. Progress on the palynostratigraphy of the Permian strata in Rio Grande do Sul State, Paraná Basin, Brazil. Anais da Academia Brasileira de Ciências 77 (2): 353-365.

Souza, P.A.; Vergel, M.M.; Beri, A. 2007. Pennsylvanian and Permian palynostratigraphy of the Paraná/ChacoParaná Basins in Brazil, Argentina and Uruguay: an integrative analysis. *In* European Meeting on the Palaeontology and Stratigraphy of Latin America, No. 4 (Díaz-Martínez, E.; Rábano, I.; editors). Instituto Geológico y Minero de España. Cuadernos del Museo Geominero 8: 361-366. Madrid.

Spalletti, L.A.; Limarino, C.O. 2006. Introduction to 'Comparison between intracratonic and active margin basins: Examples from the Late Paleozoic of western Gondwana'. Journal of South American Earth Sciences 22: 131-133.

Stollhofen, H.; Stanistreet, I.G.; Bangert, B.; Grill, H. 2000. Tuffs, tectonism and glacially related sea-level changes, Carboniferous-Permian, southern Namibia. Palaeogeography, Palaeoclimatology, Palaeoecology 161: 127-150.

Suárez, M.; de la Cruz, R.; Fanning, M.; Etchart, H. 2009. Carboniferous, Permian and Toarcian magmatism in Cordillera del Viento, Neuquén, Argentina: first U-Pb SHRIMP dates and tectonic implications. *In* Congreso Geológico Argentino, No. 17, Actas: 906-907. Jujuy.

Thomson, S.N.; Hervé, F. 2002. New time constraints for the age of metamorphism at the ancestral Pacific Gondwana margin of southern Chile (42-52°S). Revista Geológica de Chile 29 (2): 255-271.

Tohver, E.; Cawood, P.A.; Rossello, E.A.; Riccomini, C. 2007. Demise of the Gondwana ice sheet in SW Gondwana: time constraints from U-Pb zircon ages. *In* Geosur 2007: An International Congress on the Geology and Geophysics of the Southern Hemisphere, Abstract Volume: p. 163. Santiago.

Torsvik, T.H.; Cocks, R.M. 2004. Earth geography from 400 to 250 Ma: a palaeomagnetic, faunal and facies review. Journal of the Geological Society of London 161: 555-572.

Turner, B.R. 1999. Tectonostratigraphical development of the Upper Karoo foreland basin: orogenic unloading versus thermally-induced Gondwana rifting. Journal of African Earth Sciences 28 (1): 215-238.

Vaughan, A.P.M.; Storey, B.C. 2000. The eastern Palmer Land shear zone: a new terrane accretion model for the Mesozoic development of the Antarctic Peninsula. Journal of the Geological Society of London 157: 1243-1256.

Vaughan, A.P.M.; Leat, P.T.; Pankhurst, R.J. 2005. Terrane processes at the margins of Gondwana: introduction. *In* Terrane Processes at the Margins of Gondwana (Vaughan, A.P.M.; Leat, P.T.; Pankhurst, R.J.; editors). Geological Society, Special Publications 246: 1-21. London.

Veevers, J.J. 2004. Gondwanaland from 650-500 Ma assembly through 320 Ma merger in Pangea to 185-100 Ma breakup: supercontinental tectonics via stratigraphy and radiometric dating. Earth-Science Reviews 68: 1-132.

Vergel, M. 2008. Palynology of late Palaeozoic sediments (Tupe Formation) at La Herradura Creek, San Juan province, Argentina. Alcheringa: An Australasian Journal of Palaeontology 32 (4): 339-352.

Visser, J.N.J. 1996. Controls on Early Permian shelf deglaciation in the Karoo Basin of South Africa. Palaeogeography, Palaeoclimatology, Palaeoecology 125: 129-139.

Wandres, A.M.; Bradshaw, J.D.; Weaver, S.D.; Maas, R.; Ireland, T.R.; Eby, G.N. 2004. Provenance of the sedimentary Rakaia sub-terrane, Torlesse Terrane, South Island, New Zealand: the use of igneous clast compositions to define the source. Sedimentary Geology 168: 193-226.

Wandres, A.M.; Bradshaw, J.D. 2005. New Zealand tectonostratigraphy and implications from conglomeratic rocks for the configuration of the SW Pacific margin of Gondwana. *In* Terrane Processes at the Margins of Gondwana (Vaughan, A.P.M.; Leat, P.T.; Pankhurst, R.J.; editors). Geological Society, Special Publications 246: 179-216. London.

Willan, R.C.R. 2003. Provenance of Triassic-Cretaceous sandstones in the Antarctic Peninsula: implications for terrane models during Gondwana breakup. Journal of Sedimentary Research 73 (6): 1062-1077.

Williams, I.S. 1998. U-Th-Pb geochronology by ion microprobe. *In* Applications of microanalytical techniques to understanding mineralizing processes (McKibben, M.A.; Shanks, W.S. III; Ridley, W.I.; editors). Reviews in Economic Geology 7: 1-35.

Willner, A.P.; Sepúlveda, F.A.; Hervé, F.; Massonne, H.-J.; Sudo, M. 2009. Conditions and timing of pumpellyite-actinolite-facies metamorphism in the Early Mesozoic frontal accretionary prism of the Madre de Dios Archipelago (Latitude 50°20'S; Southern Chile). Journal of Petrology 50 (11): 2127-2155.

Manuscript received: December 22, 2008; revised/accepted: January 13, 2010.